

Aus der medizinischen Klinik und Poliklinik II  
der Universität Würzburg  
Direktor: Professor Dr. med. Hermann Einsele

## **Zinc homeostasis in megakaryocytes**

Studien zur Expression und Regulation von Zink-Transportern in  
Megakaryozyten

### **Inauguraldissertation**

zur Erlangung der Doktorwürde der

Medizinischen Fakultät

der

Julius-Maximilians-Universität Würzburg

vorgelegt von

**Leonard Wagner**

aus Würzburg

**Würzburg, Oktober 2019**



**Referent: Prof. Dr. med. Andreas Geier**

**Korreferent: Prof. Dr. rer. nat. Bernhard Nieswandt**

**Dekan: Prof. Dr. Matthias Frosch**

**Tag der mündlichen Prüfung: 25.09.2020**

**Der Promovend ist Zahnarzt.**

# Table of Contents

1. Introduction .....	1
1.1 Systemic Zn <sup>2+</sup> homeostasis .....	1
1.1.1 Organismal Zn <sup>2+</sup> uptake and release in physiological conditions .....	1
1.1.2 Imbalanced zinc homeostasis and its consequences .....	2
1.2 Cellular Zn <sup>2+</sup> homeostasis .....	4
1.2.1 Intracellular Zn <sup>2+</sup> stores .....	4
1.2.2 Regulation of Zn <sup>2+</sup> influx by ZIP transporters ( <i>Slc39a</i> ) .....	5
1.2.3 Regulation of Zn <sup>2+</sup> efflux by zinc transporter ZnT ( <i>Slc30a</i> ) .....	10
1.3 Megakaryopoiesis and platelet production .....	13
1.4 Regulation of Zn <sup>2+</sup> homeostasis in megakaryocytes and platelets .....	15
1.4.1 Zn <sup>2+</sup> homeostasis in megakaryocytes .....	15
1.4.2 Zn <sup>2+</sup> homeostasis in platelets .....	15
1.5 Aim of Studies .....	16
2. Materials and Methods .....	17
2.1 Materials .....	17
2.1.1 Cell culture material .....	17
2.1.2 Mouse models .....	17
2.1.3 RNA extraction material .....	18
2.1.4 cDNA synthesis material .....	18
2.1.5 Real time polymerase chain reaction material .....	18
2.1.6 RT-PCR primer .....	19
2.1.7 Technical equipment .....	21
2.1.8 Software .....	21
2.2 Methods .....	22
2.2.1 Extraction of murine bone marrow cells .....	22
2.2.2 Culturing of megakaryocytes .....	22
2.2.3 Stimulation of megakaryocytes during megakaryopoiesis .....	22
2.2.4 Purification of megakaryocytes .....	22
2.2.5 Stimulation of matured megakaryocytes .....	23

2.2.6 Collecting of cells during all stages of megakaryopoiesis .....	23
2.2.7 RNA purification .....	23
2.2.8 Measurement of RNA concentration .....	24
2.2.9 cDNA synthesis .....	24
2.2.10 Primer design .....	25
2.2.11 Real time polymerase chain reaction (RT-PCR) .....	25
2.2.12 Statistical methods .....	27
3. Results.....	28
3.1 <i>In vitro</i> cultivation of primary mouse megakaryocytes .....	28
3.1.2 Cellular Zn <sup>2+</sup> toxicity in primary mouse megakaryocytes .....	28
3.1.3 Zn <sup>2+</sup> chelator TPEN inhibits megakaryopoiesis .....	30
3.2 Expression profile of <i>Slc39a</i> genes in mature megakaryocytes .....	32
3.2.1 Regulation of <i>Slc39a1</i> (ZIP1) .....	33
3.2.2 Regulation of <i>Slc39a3</i> (ZIP3) .....	35
3.2.3 Regulation of <i>Slc39a4</i> (ZIP4) .....	36
3.2.4 Regulation of <i>Slc39a6</i> (ZIP6) .....	37
3.2.5 Regulation of <i>Slc39a7</i> (ZIP7) .....	38
3.2.6 Regulation of <i>Slc39a9</i> (ZIP9) .....	39
3.2.7 Regulation of <i>Slc39a10</i> (ZIP10) .....	40
3.2.8 Regulation of <i>Slc39a11</i> (ZIP11) .....	41
3.3 Expression profile of <i>Slc30a</i> genes in mature megakaryocytes .....	43
3.3.1 Regulation of <i>Slc30a1</i> (ZnT1) .....	44
3.3.2 Regulation of <i>Slc30a5</i> (ZnT5) .....	46
3.3.3 Regulation of <i>Slc30a6</i> (ZnT6) .....	47
3.3.4 Regulation of <i>Slc30a7</i> (ZnT7) .....	48
3.3.5 Regulation of <i>Slc30a9</i> (ZnT9) .....	49
4. Discussion .....	51
4.1 Extracellular Zn <sup>2+</sup> concentration strongly influences megakaryopoiesis ..	51
4.2 Transcriptional expression of genes encoding for ZIP proteins in MKs ..	52
4.3 Transcriptional expression of genes encoding for ZnT proteins in MKs ..	55
4.5 Outlook.....	56

5. Summary .....	57
5. Zusammenfassung .....	58
6. References .....	60
7. List of Figures .....	70
8. Appendix.....	71
8.1 RT-PCR primer test based on the example of <i>Slc30a1</i> in liver tissue .....	71
8.2 Publication .....	72

# 1. Introduction

## 1.1 Systemic Zn<sup>2+</sup> homeostasis

### 1.1.1 Organismal Zn<sup>2+</sup> uptake and release in physiological conditions

Zinc (Zn<sup>2+</sup>) is an essential trace metal element in all organisms and serves as an important component of metabolic pathways, as a structural component of zinc finger or LIM domains, but also as an important signaling molecule. Zn<sup>2+</sup> has important catalytic functions by stabilizing negative charges in biochemical reactions in over 300 enzymes. Cellular Zn<sup>2+</sup> uptake can increase the enzymatic activity of mitogen-activated protein kinase (MAPK), caspases, metalloproteinases and other enzymes. Zn<sup>2+</sup> is responsible for maintaining the protein structure in zinc-finger-transcription factors thus Zn<sup>2+</sup> can be coordinated by oxygen, sulfur and nitrogen atoms of the polypeptide chain. Many secretory cells, such as pancreatic  $\beta$ -cells, neutrophils, and platelets can release a significant amount of Zn<sup>2+</sup> to influence diverse Zn<sup>2+</sup> dependent processes in the blood plasma (1-3).

Healthy adult men store approximately 2-3g Zn<sup>2+</sup> in the body, but require 10-15 mg nutritional Zn<sup>2+</sup> uptake per day to maintain physiological organ function (4). Zn<sup>2+</sup> is absorbed in the small intestine; mainly in the jejunum (5). The transporter responsible for the uptake of dietary Zn<sup>2+</sup> is ZIP4. Located at the apical membrane, it facilitates the transport of Zn<sup>2+</sup> from the intestinal lumen into the cytosol of enterocytes. To maintain physiological plasma Zn<sup>2+</sup> concentrations, this process is regulated precisely. Zn<sup>2+</sup> deficiency leads to stabilization of ZIP4 mRNA and therefore accumulation of the protein at the apical membrane, leading to improved Zn<sup>2+</sup> uptake. Under excess conditions, ZIP4 is internalized rapidly, ubiquitinated and degraded in the proteasome. The Zn<sup>2+</sup> absorbed by the enterocytes is then thought to be released into the bloodstream by Zn<sup>2+</sup> transporter ZnT1 located at the basolateral membrane (6).

Under physiological conditions, excess Zn<sup>2+</sup> is mainly excreted via the feces, however the exact regulatory mechanisms are yet to be enlightened. Renal

excretion and loss of  $Zn^{2+}$  via integument play a secondary role, only under extreme conditions the amount of  $Zn^{2+}$  excreted into urine is altered (7).  $Zn^{2+}$  is mainly stored intracellularly in skeletal muscle (60%) and bone (30%). Only residual amounts of this  $Zn^{2+}$  pool (0.1%) are located in the blood plasma. Under physiological conditions, the total plasma concentration of  $Zn^{2+}$  in humans ranges from 10 to 20  $\mu M$ , but the majority of the plasma resident  $Zn^{2+}$  is covalently linked to albumin and  $\alpha_2$ -macroglobulin (8, 9).

### 1.1.2 Imbalanced zinc homeostasis and its consequences

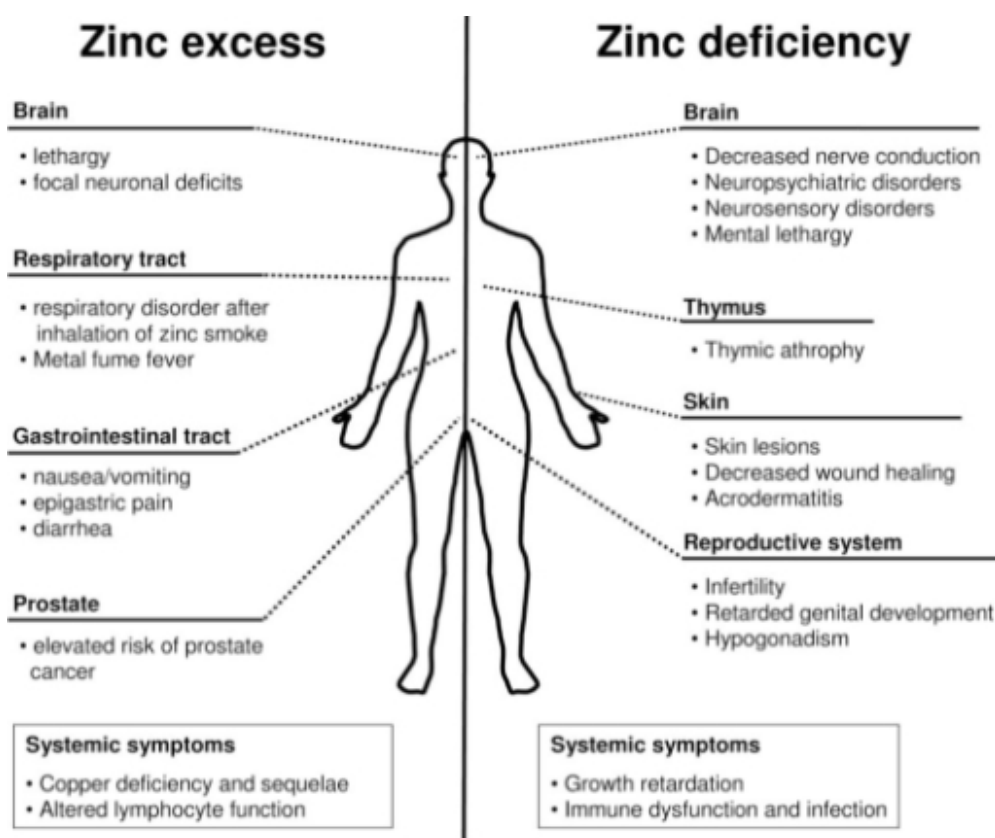


**Figure 1.** Dysregulated zinc uptake or release induces multiple defects in several organs of the human body. Chart (Creative Commons license) from Plum et al. (10)

#### 1.1.2.1 $Zn^{2+}$ deficiency and human diseases

$Zn^{2+}$  deficiency is a widespread phenomenon in developing countries and induces multiple metabolic defects in different organs. The main reason for

deficiency is a diet high on phytate, a metal ion chelator that impedes  $Zn^{2+}$  absorption in the intestine. In the brain, lack of  $Zn^{2+}$  is associated with decreased nerve conduction, neuropsychiatric disorders like depression, neurosensory disorders and mental lethargy. Size and function of the thymus is reduced in children suffering from  $Zn^{2+}$  deficiency, leading to reduced lymphocyte counts and therefore to serious immune dysfunction. Wound healing and skin integrity are affected in a negative way as well. Impaired  $Zn^{2+}$  absorption in the intestine due to a defect in the *SLC39A4* gene encoding for ZIP4 leads to the characteristic syndrome of *Acrodermatitis enteropathica*. Dwarfism, hypogonadism, and infertility are linked to  $Zn^{2+}$  deficiency as well (10).

Under pathophysiological conditions, cellular  $Zn^{2+}$  deficiency is strongly associated with cell cycle arrest and apoptosis.  $Zn^{2+}$  depletion induced by  $Zn^{2+}$  chelator N,N,N',N'-tetrakis(2-pyridylmethyl)ethylenediamine (TPEN) activates Caspase-3, thereby triggering the apoptotic cascade (11). On the other hand,  $Zn^{2+}$  supplementation inhibits apoptosis by increasing the Bcl-2/Bax ratio in the cell (12).

### **1.1.2.2 $Zn^{2+}$ overload and human diseases**

Due to very effective mechanisms of systemic  $Zn^{2+}$  homeostasis,  $Zn^{2+}$  overload is very unlikely. However, in extreme conditions, excess  $Zn^{2+}$  nevertheless has toxic effects. Inhalation of  $Zn^{2+}$  containing smoke can lead to adult respiratory distress syndrome (ARDS) and metal fume fever, both diseases mostly experienced by  $Zn^{2+}$  processing industrial workers. When toxic amounts of  $Zn^{2+}$  were taken in orally, patients suffered from gastrointestinal symptoms like nausea, vomiting, epigastric pain, and diarrhea. Neuronal deficits and lethargy were reported for  $Zn^{2+}$  intoxication as well. However, the most important effect of continuous  $Zn^{2+}$  excess is that copper resorption in the intestine is impaired, leading to copper deficiency and its sequelae like anemia, leukopenia, neutropenia, and abnormal cardiac function. Furthermore,  $Zn^{2+}$  excess inhibited lymphocyte function (10).

The severe consequences of  $Zn^{2+}$  excess and deficiency highlight the importance of tight regulation of  $Zn^{2+}$  homeostasis for physiological organ function.



## 1.2 Cellular Zn<sup>2+</sup> homeostasis

### 1.2.1 Intracellular Zn<sup>2+</sup> stores

Cellular Zn<sup>2+</sup> is located in the nucleus, cytoplasm, endoplasmic reticulum (ER), Golgi, and also stored in vesicles or secretory granules. The amount of metabolically active Zn<sup>2+</sup> is very limited in the cell because of its cytotoxicity. Therefore, the majority of Zn<sup>2+</sup> is immediately transported and stored during cellular Zn<sup>2+</sup> uptake. Most of the Zn<sup>2+</sup> is sequestered by metalloproteins called metallothioneins in the cytoplasm. Metallothioneins (MT) are a small group of cysteine-rich polypeptides, complexing up to seven Zn<sup>2+</sup> ions and sequester this Zn<sup>2+</sup> pool in the cytoplasm. Depending on the cell type and activation state of the cell, approximately 5-15% of cytoplasmic Zn<sup>2+</sup> can bind to MT. When the sulfur group of MT is oxidized, they lose their ability to bind zinc, and this process enhances Zn<sup>2+</sup> release by MT (2). Enhanced Zn<sup>2+</sup> uptake induces MT gene expression by metal transcription factor 1 (MTF-1), thereby increasing the storage capacity of Zn<sup>2+</sup> in the cell (13).

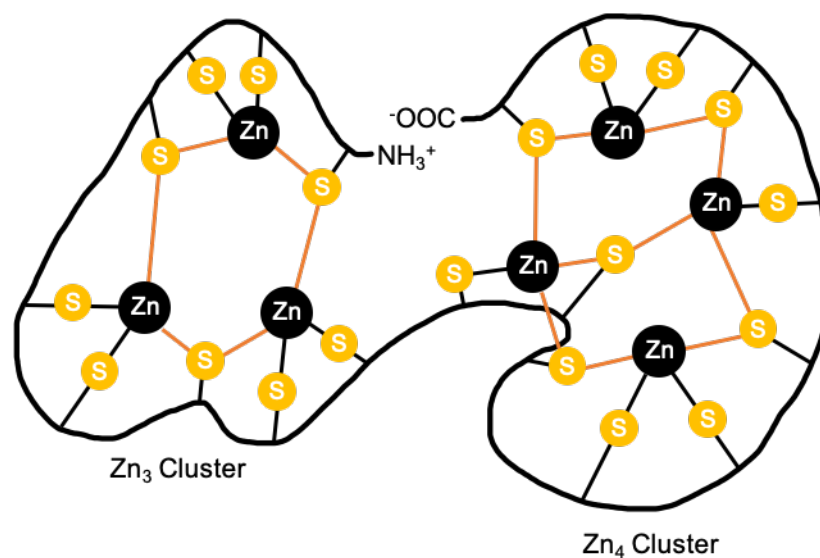


**Figure 2.** Schematic picture of metallothionein thiolate clusters binding to Zn<sup>2+</sup>. Adapted after Fischer and Davie (14).

Alternatively, Zn<sup>2+</sup> can also be stored in secretory vesicles and granules, ER, mitochondria, and Golgi. The phospholipid membrane of the intracellular store is

impermeable for  $Zn^{2+}$ . Therefore, cells need to express several  $Zn^{2+}$  transporters to facilitate and regulate the ions store content in the cellular organelles.

### **1.2.2 Regulation of $Zn^{2+}$ influx by ZIP transporters (*Slc39a*)**

Solute Carriers are a group of transmembrane proteins that regulate cellular ion transport in various cell types. More than 400 protein members have been identified so far, many of them facilitate metal transport across the plasma and intracellular membranes. Depending on sequence similarities, they are classified into different families and subfamilies. Typically, solute carriers contain several  $\alpha$ -helices that span the membrane (15).

The *Slc39a* Family was named ZIP (**Z**rt, **I**rt- related **p**rotein), after the first two known members *Irt1* of *Arabidopsis thaliana* and *Zrt1* of *Saccharomyces cerevisiae*. The family members have eight predicted transmembrane  $\alpha$ -helices. The amino- and the carboxy-terminal ends are thought to be located on the luminal or extracellular side of the membrane. The exact structure of mammalian ZIPs has not been established. So far, 14 human ZIPs as well as their 14 murine homologues have been isolated and characterized (16).

ZIP family members transport  $Zn^{2+}$  from the extracellular space or from the lumen of cellular organelles or vesicles into the cytoplasm, thereby increasing the levels of cytoplasmic  $Zn^{2+}$ . Some of these Transporters are not strictly specific for zinc, other metals such as iron, copper, cadmium and manganese could be transported as well, depending on the physiological status of the cell. Various mechanisms of transport regulation are reported for ZIPs: Up- and downregulation of gene expression for some members of the ZIP family, a mechanism of translocating the protein from vesicles proximal to the membrane into the cell membrane under  $Zn^{2+}$  deficient conditions, and vice versa, a mechanism of internalization and degradation of the protein under zinc excess conditions and regulation on translational level. (2)

In the following, all 14 mammalian ZIP family members are introduced shortly.

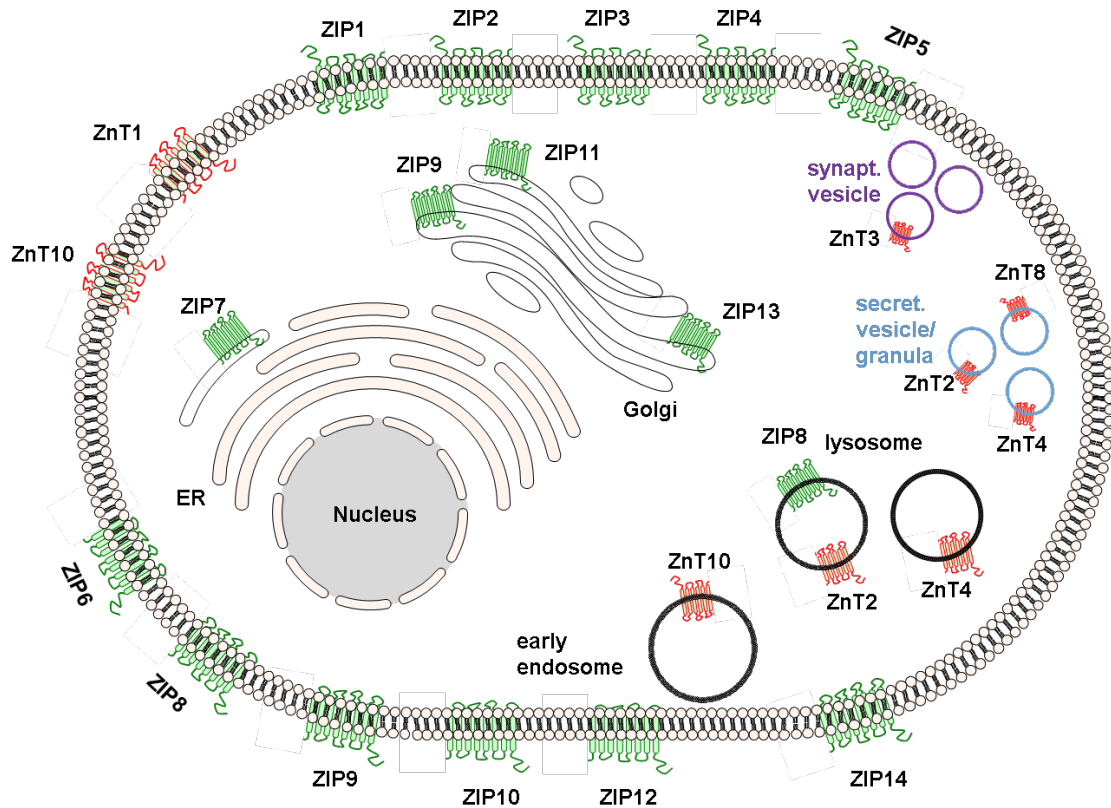


**Figure 3.** Subcellular localization of selected ZIP and ZnT transporters in mammalian cells. Figure created by PD Dr. Heike Hermanns.

### ZIPII subfamily

**ZIP1 (*Slc39a1*)** is located at the plasma membrane and responsible for the uptake of  $Zn^{2+}$  from the extracellular space. Binding of other metals such as cadmium, iron or copper leads to ZIP1 endocytosis. Therefore,  $Zn^{2+}$  uptake can be decreased under pathological conditions. However,  $Zn^{2+}$  binding to ZIP1 is quite substrate specific under physiological conditions. The *Slc39a1* gene encodes for ZIP1, which is widely expressed in human and mouse tissues, but mRNA or protein expression of the gene is not thought to be influenced by cellular zinc status (17-19). *Slc39a1* knockout mice exhibit normal fertility and postnatal development on a zinc-adequate diet. In contrast, when feeding pregnant mice a  $Zn^{2+}$  deficient diet knockout embryos more frequently develop abnormalities compared to wild type embryos (20).

**ZIP2 (*Slc39a2*)** has very similar characteristics to ZIP1 concerning its localization at the cell membrane and the substrate specificity to  $Zn^{2+}$ . However, its gene expression profile is restricted to a few organs, such as liver and skin. Upregulation of the *Slc39a2* gene under  $Zn^{2+}$  deficient conditions was reported in THP-1 monocytes. *Slc39a2* knockout mice have normal postnatal development when fed with zinc-replete diet. However,  $Zn^{2+}$  deficiency of pregnant mice results in impaired growth with craniofacial and limb defects, and show altered  $Fe^{2+}$  and  $Ca^{2+}$  levels (17, 21, 22).

**ZIP3 (*Slc39a3*)** shares many physiological properties with ZIP1, including its location at the plasma membrane as well as endosomal trafficking and protein degradation in disease state of  $Zn^{2+}$  excess. So far, *Slc39a3* gene expression appears not to be influenced by  $Zn^{2+}$  status, but only limited studies have been published due to restricted gene expression of *Slc39a3*. ZIP3 is mainly detected in testes, although low expression level was also detected in other tissues, similarly to ZIP2 (17, 18). *Slc39a3* knockout mice stressed with  $Zn^{2+}$  deficient diet during pregnancy exhibit a high frequency to develop abnormal morphogenesis of the embryo. Numbers of thymic pre-T cells were strongly reduced indicating an important role in the development of the immune system (23).

In summary, knockout mice of all three ZIPII subfamily members showed abnormal embryonic development under  $Zn^{2+}$  limited conditions. So far, human disorders have not been associated with this ZIP subfamily (20, 21, 23, 24).

#### **LIV-1 subfamily**

**ZIP4 (*Slc39a4*)** is located at the apical membrane of enterocytes and therefore crucial for absorption of dietary  $Zn^{2+}$  in the small intestine. ZIP4 imports  $Zn^{2+}$  from the intestinal lumen into the cell. Gene expression of *Slc39a4* is high in the intestine, but rather low in other organs. It has been shown that  $Zn^{2+}$  deficiency induces gene expression of *Slc39a4*, while  $Zn^{2+}$  overload leads to internalization and degradation of the ZIP4 protein. *Acrodermatitis enteropathica*, a rare hereditary disease is associated with mutation of *Slc39a4*. Because of the

impaired  $Zn^{2+}$  absorption in the intestine, patients suffer from dermatitis, alopecia and diarrhea. *Slc39a4* knockout mice die in utero during embryonic development around E10 indicating an essential role of ZIP4 in organismal  $Zn^{2+}$  homeostasis (25-29).

**ZIP5 (*Slc39a5*)** has been detected only in small intestine, liver and pancreas. The ZIP5 protein is located at the basolateral membrane of polarized cells. Gene expression of *Slc39a5* is independent of  $Zn^{2+}$  status of the body. However, ZIP5 function is regulated on protein level, since  $Zn^{2+}$  excess increases the protein level in the basolateral membrane. *Slc39a5* knockout mice display an impaired hepatic and pancreatic  $Zn^{2+}$  homeostasis, associated with an increased susceptibility to develop zinc-induced pancreatitis (26, 30-32).

**ZIP6 (*Slc39a6*)**, also known as LIV-1, is located in the plasma membrane and its function is regulated by sex steroid hormones in mammary gland and prostate. Gene expression of *Slc39a6* indeed can be enhanced by estrogen or STAT3. Overexpression of *Slc39a6* is associated with migration of breast cancer cells. Lymphocytes isolated from *Slc39a6* knockout mice showed no alteration in zinc transport or proliferation under resting conditions, but after activation knockout lymphocytes showed deficient  $Zn^{2+}$  transport, thereby inhibiting diverse cellular responses to receptor stimuli (33-35).

**ZIP7 (*Slc39a7*)** is ubiquitously expressed in human tissues and localized in the membranes of the Golgi apparatus and ER. Gene expression of *Slc39a7* is independent of the  $Zn^{2+}$  status. However, the protein level of ZIP7 is decreased when zinc is highly abundant. ZIP7 plays an important role in cellular zinc signaling. When ZIP7 releases  $Zn^{2+}$  from the ER or Golgi, increase of  $Zn^{2+}$  level induces phosphorylation cascades of ERK and AKT. *Slc39a7* overexpression is frequently observed in breast cancer. Conditional inactivation of *Slc39a7* in intestinal epithelial cells exhibit premature death, loss of epithelial integrity reduced enterocyte proliferation and increased enterocyte apoptosis in the gut, suggesting an essential role of ZIP7 in systemic  $Zn^{2+}$  homeostasis (36-39).

**ZIP8 (*Slc39a8*)** is a non-selective metal transporter, binding to  $Zn^{2+}$ ,  $Fe^{2+}$ ,  $Cd^{2+}$ , and  $Mn^{2+}$  and is located in the plasma membrane of lysosomes. Increase of ZIP8 level in the plasma membrane was observed under  $Zn^{2+}$  deficiency. Neonates of *Slc39a8* knockout mice die, indicating an important role of ZIP8 mediated cation uptake in hematopoiesis and organogenesis (40-44).

**ZIP10 (*Slc39a9*)** is located in the plasma membrane and selectively transports  $Zn^{2+}$  from the extracellular space into the cytoplasm.  $Zn^{2+}$  deficiency leads to increased gene expression of *Slc39a10* while  $Zn^{2+}$  excess downregulates the mRNA levels. *Slc39a10* is regulated by JAK/STAT and MTF-1 signaling pathways. ZIP10 overexpression is associated with altered invasiveness of cancer cells. Mice with conditional loss of function display defects in cellular proliferation and differentiation (45-48).

**ZIP12 (*Slc39a12*)** is located in intracellular and plasma membranes; high expression levels were detected in the brain. Under  $Zn^{2+}$  deficient conditions, the ZIP12 protein migrates from intracellular membranes to the plasma membrane to enhance  $Zn^{2+}$  uptake. ZIP12 function is crucial for neuronal cell differentiation (49).

**ZIP13 (*Slc39a13*)** is located in the membranes of the Golgi apparatus. Gene expression of *Slc39a13* is regulated independently from the cellular  $Zn^{2+}$  status. ZIP13 is highly expressed in connective tissues. Genetic mutation of *Slc39a13* in human patients accounts for the development of spondylocheiro dysplastic form of the Ehlers-Danlos syndrome. These patients suffer from abnormal development of bones, cartilage and teeth. *Slc39a13* knockout mice develop similar pathological symptoms with skeletal and dental abnormalities, indicating evolutionary conserved organismal functions of ZIP13 in humans and mice (50, 51).

**ZIP14 (*Slc39a14*)** a non-selective metal transporter, binding to  $Zn^{2+}$ ,  $Fe^{2+}$ ,  $Cd^{2+}$  and  $Mn^{2+}$  and located at the surface of the cell. ZIP14 is highly expressed in the liver. is a cell-surface localized metal transporter highly expressed in the liver.  $Zn^{2+}$  depletion or inflammatory conditions triggered by IL-6 leads to upregulation of *Slc39a14*. Iron deficiency leads to downregulation and protein degradation of ZIP14. *Slc39a14* knockout mice show impaired skeletal growth, and multiple defects in several organs, such as dwarfism, scoliosis, osteopenia, short long bones, altered gluconeogenesis and chondrocyte differentiation. In the liver,  $Zn^{2+}$  level is reduced thereby inhibiting hepatocyte proliferation after hepatectomy (52-56).

#### **ZIPI subfamily**

**ZIP9 (*Slc39a9*)** is a specific  $Zn^{2+}$  transporter located in the Golgi apparatus and plasma membrane and the only known member of the ZIPI subfamily. Zinc status of the body does not influence gene expression of *Slc39a9* or subcellular localization of ZIP9. Functions of ZIP9 can be activated by androgen hormones (57, 58).

#### **GufA subfamily**

**ZIP11 (*Slc39a11*)** is the only transporter assigned to the *gufA*- subfamily. *Slc39a11* is abundantly expressed in stomach and colon. ZIP11 is intracellularly localized in nucleus and plasma membrane.  $Zn^{2+}$  status slightly changes gene activity of *Slc39a11* (59, 60).

#### **1.2.3 Regulation of $Zn^{2+}$ efflux by zinc transporter ZnT (*Slc30a*)**

Members of *Slc30a* gene family are selective  $Zn^{2+}$  transporters located at the cell surface and in membranes of intracellular organelles. Several *Slc30a* genes and ZnT proteins were identified in mouse and human, according to similar gene structure or amino acid alignments, respectively. ZnT proteins can reduce the intracellular  $Zn^{2+}$  concentrations by pumping out the cytoplasmic  $Zn^{2+}$  to the extracellular space or into intracellular organelles, such as secretory granules, lysosomes, Golgi or ER. With one exception, ZnT proteins have six predicted

transmembrane domains and both N- and C- termini are located at the cytosolic side of the membrane. ZnT usually form homodimers and reduce  $Zn^{2+}$  levels using an  $H^+/Zn^{2+}$ - antiport mechanism. (2)

**ZnT1 (*Slc30a1*)** was the first described mammalian  $Zn^{2+}$  transporter. ZnT1 plays an important role in protecting cells from  $Zn^{2+}$  overload, therefore the gene expression of *Slc30a1* is upregulated under  $Zn^{2+}$  excess conditions. Interestingly,  $Zn^{2+}$  deficiency does not alter gene expression of *Slc30a1*. In general, ZnT1 is mainly located to the plasma membrane but another cellular distribution has been reported as well. Increase of *Slc30a1* expression is regulated by activation of Raf-1 kinase signaling. *Slc30a1* knockout mice die during early embryonic development and embryos from heterozygous females on a zinc deficient diet develop abnormally, indicating a very important role of ZnT1 in organismal  $Zn^{2+}$  homeostasis (61-66).

**ZnT2 (*Slc30a2*)** has two splice variants, the long one is located in the membrane of secretory vesicles, the short one in the plasma membrane. It enriches vesicles with  $Zn^{2+}$ , making the cell more resistant to excess of zinc. *Slc30a2* gene expression is upregulated via STAT5. The transporter plays an important role in secreting zinc into milk during lactation. Mice homozygous for *Slc30a2* allele exhibit abnormal mammary gland development during lactation, abnormal  $Zn^{2+}$  levels in the mammary gland and milk, impaired lactation and decreased litter survival (67-70).

**ZnT3 (*Slc30a3*)** is mainly expressed in the central nervous system and is responsible for  $Zn^{2+}$  transport into synaptic vesicles. Targeting of the protein to the vesicles is modulated by an adaptor protein. Knockout of the gene leads to limitations in brain function in mice. While  $Zn^{2+}$  is absent from synaptic vesicles of knockout neurons, inactivation of *Slc30a3* does not affect brain development or cellular morphology. (71, 72)



**ZnT4 (Slc30a4)** is a ubiquitously expressed Zn<sup>2+</sup> transporter localized in the secretory pathway including the Golgi as well as cytoplasmic vesicles. Subcellular localization of the ZnT4 changes in response to Zn<sup>2+</sup> status. Mutation of *Slc30a4* leads to the phenotype of the lethal milk mouse, dramatically decreasing the amount of Zn<sup>2+</sup> in murine breast milk which is lethal to nursing pups. Pleiotropic defects have been observed in *Slc30a4* knockout mice, including otolith degeneration, impaired motor coordination alopecia, and dermatitis. Mutation of ZnT4 in human patients does not show an equivalent phenotype indicating species differences in the cellular functions of ZnT4 between mammals. (73-77)

**ZnT5 (Slc30a5)** is mainly localized in the Golgi apparatus. In contrast to other ZnT proteins which form homodimers, ZnT5 forms heterodimers with ZnT6. Gene expression of *Slc30a5* is upregulated under Zn<sup>2+</sup> deficiency while Zn<sup>2+</sup> excess does not change expression of the gene. *Slc30a5* knockout mice show abnormal bone development with osteopenia including reduced bone density. The majority of adult knockout males die suddenly due to severe bradyarrhythmia, but females have a normal life span (66, 78-80).

**ZnT6 (Slc30a6)** forms heterodimers with ZnT5 and localizes to the Golgi membrane. ZnT6 does not directly transport Zn<sup>2+</sup> since it lacks the characteristic Zn<sup>2+</sup> binding site. Therefore, ZnT6 was proposed to be only a modulator of ZnT5. In response to excess Zn<sup>2+</sup>, ZnT6 leaves the Golgi apparatus and accumulates in the plasma (73, 79, 81).

**ZnT7 (Slc30a7)** protein is a transporter that mediates zinc influx into the Golgi. Excess Zn<sup>2+</sup> does not influence mRNA expression of *Slc30a7* significantly. However, Zn<sup>2+</sup> deficit induced by TPEN increases the expression level. Mice homozygous for a gene trapped allele exhibit a low body zinc status, reduced food intake, and poor body weight gain, and are lean due to a significant reduction in body fat accumulation. However, no signs of hair growth abnormalities or dermatitis, typical symptoms of Zn<sup>2+</sup> deficiency, were observed (66, 82, 83).

**ZnT8 (*Slc30a8*)** is a Zn<sup>2+</sup> transporter specifically expressed in the Langerhans islets of the pancreas and is tightly associated with insulin secretion. ZnT8 is localized in the membrane of insulin secretory vesicles. Expression of *Slc30a8* is regulated by transcription factor Pdx-1. Knockout mice of *Slc30a8* exhibit a low body Zn<sup>2+</sup> status which leads to disrupted insulin secretion, reduced food intake, and poor body weight gain (3, 84-87).

**ZnT9 (*Slc30a9*)**, also named GAC63/HUEL was assigned to the *Slc30a* family because of sequence similarities in the cation efflux domain of ZnT9 to other ZnT family members. However, it has never been confirmed that ZnT9 is capable of transporting Zn<sup>2+</sup>. Instead, a role as a nuclear receptor coactivator was suggested (88-90).

**ZnT10 (*Slc30a10*)** is localized in the plasma membrane, Golgi, and early endosomes. The subcellular localization is influenced by Zn<sup>2+</sup> abundance. *Slc30a10* is highly expressed in only few tissues and downregulated by IL-6. However, ZnT10 plays an important role in manganese homeostasis as well (91-94).

### **1.3 Megakaryopoiesis and platelet production**

At the beginning of the 20th century, Wright described Megakaryocytes (MKs) as the precursor cells of platelets (95). MKs are located mainly in the bone marrow and spleen and differentiate from hematopoietic stem cells. Megakaryopoiesis is tightly regulated by various transcription factors. Hematopoietic stem cells are the progenitors of all blood cells. They commit either to the lymphoid or to the myeloid lineage. Under the control of transcription factor GATA-1, myeloid progenitors develop to megakaryocyte-erythroid progenitor cells which are further differentiated to megakaryocyte progenitors (96). At the earliest stage, the size of these progenitor cells is approximately 10-15µm in diameter and they already express megakaryocyte-specific markers like the integrin αIIb and the glycoprotein GPIbα at low levels. At later stage, MKs increase the size via

endomitosis and increase their nuclei number up to 128 N, thus the final size of MKs reaches 40-60µm. During endomitosis MKs can synthesize and accumulate huge amounts of membranes, organelles and proteins during their maturation process to be capable of producing 1,000 - 5,000 platelets per cell. The demarcation membrane system is the first example of a megakaryocyte-specific organelle. It consists of a large pool of tubular invaginations of the plasma membrane and serves as a membrane reservoir for the formation of proplatelets. Platelet granules are formed in the MK cytoplasm. Platelets do not have a nucleus or nuclear DNA, and *de novo* protein translation is also limited. Therefore, all organelles and proteins mainly derive from the mother MK cell. Mature MKs start to release proplatelets into the sinusoid vessels of the bone marrow. Under shear force of the bloodstream, proplatelets are shed into the blood, where proplatelets undergo their final development to fully functional platelets (97-99).

Three major groups of platelet granules are found in the cytosol: α-granules, δ-granules, and few lysosomes. In addition, few mitochondria located in the platelet body maintain energy metabolism. In α-granules, the membrane proteins ItgαIIb and GPIbα, coagulation factors V, IX, and XIII, fibrinogen, and von-Willebrand factor as well as chemokines and growth factors have been identified. In δ-granules, high concentrations of ions, such as Ca<sup>2+</sup>, Mg<sup>2+</sup>, and K<sup>+</sup>, pyrophosphates and also serotonin, histamine and nucleotides are located. Platelet granule release plays an important role in physiological and pathological conditions. Impaired granule biogenesis or abnormal granule release strongly influence hemostasis, as observed in storage-pool disorders (100-102).

The main regulator of Megakaryocytopoiesis and platelet production is a cytokine called thrombopoietin (TPO). The gene of TPO is widely expressed in mammalian tissues, the highest expression levels are found in the liver. Platelets internalize and metabolize TPO from the blood plasma, decreasing the total concentration of the protein. Under thrombocytopenic conditions, due to the reduced platelet count, TPO concentration strongly increases in the bone marrow thereby inducing MK differentiation and proplatelet formation. TPO stimulates MK differentiation from hematopoietic stem cells by binding to the c-Mpl-Receptor and downstream activation of JAK2, STAT3 and STAT5 as well as the Raf-1/MAP

kinase pathway (103). Under *in vitro* conditions TPO can effectively induce megakaryopoiesis from hematopoietic stem cells isolated from the bone marrow (104).

## **1.4 Regulation of Zn<sup>2+</sup> homeostasis in megakaryocytes and platelets**

### **1.4.1 Zn<sup>2+</sup> homeostasis in megakaryocytes**

After extensive literature search, only very limited information about Zn<sup>2+</sup> homeostasis in MKs was found. Earlier, metallothionein (MT) was investigated in human megakaryocytes. Seven isoform-specific mRNAs namely MT-1A, MT-1B, MT-1E, MT-1G, MT-1H, MT-1X, and MT-2A were detected in MKs and 100µM of zinc supplement could induce upregulation of total MT transcripts in MKs at 48 h post-treatment. This preliminary data suggests that MT seems to be an important Zn<sup>2+</sup> store in the cytoplasm of MKs (105). However, the molecular mechanism of Zn<sup>2+</sup> uptake and release has not been investigated in this cell type.

### **1.4.2 Zn<sup>2+</sup> homeostasis in platelets**

Platelets can release significant amounts of Zn<sup>2+</sup> from α-granules upon activation, increasing the local concentration of extracellular Zn<sup>2+</sup> up to 10µM (106). Zn<sup>2+</sup> enhances factor XII autoactivation and activation mediated by kallikrein, promoting coagulation via the intrinsic pathway (107). On the platelet surface, the presence of Zn<sup>2+</sup> facilitates binding of factor XI to GPIbα. The activated form of factor XI then promotes factor IX activation and the formation of the tenase complex, enhancing further downstream thrombin activation and fibrin formation (108). Consequently, Zn<sup>2+</sup> deficiency could strongly influence the coagulation cascade and fibrin formation leading to prolonged bleeding times in human, mouse and rat (109, 110). Platelet aggregation is enhanced in the presence of Zn<sup>2+</sup>, because it mediates binding of fibrinogen to the platelet fibrinogen receptor integrin αIIb, and therefore enhances the binding of the platelets to the fibrin clot (111). Zn<sup>2+</sup> status of the cells also regulates Ca<sup>2+</sup> homeostasis. Ca<sup>2+</sup> is mainly stored in the dense tubular system, but also in δ-granules of platelets. Intracellular Ca<sup>2+</sup> mobilization is crucial for platelet degranulation, aggregation and coagulation. Impaired Ca<sup>2+</sup> uptake of platelets as a consequence of Zn<sup>2+</sup>

deficiency could be a factor of bleeding complications in humans, although the exact mechanism of how  $Zn^{2+}$  influences platelet  $Ca^{2+}$  homeostasis has not yet been established (112, 113).  $Zn^{2+}$  directly binds fibrinogen and fibrin, thereby enhancing fibrin clot formation by changing the ultrastructure of fibrin during polymerization (114, 115). Altogether, these results highlight the dynamic role of  $Zn^{2+}$  in platelet activation, coagulation, and fibrin clot formation.

### **1.5 Aim of Studies**

Although platelet  $\alpha$ -granule resident  $Zn^{2+}$  release contributes to hemostasis, the molecular mechanisms of  $Zn^{2+}$  influx and efflux in platelets are not entirely understood today. Accumulation of free ionic  $Zn^{2+}$  was observed in secretory granules of MKs and platelets, indicating the existence of a complex  $Zn^{2+}$  transport system. Resting platelets incubated with extracellular  $Zn^{2+}$  rapidly increase their intracellular  $Zn^{2+}$  levels, suggesting that platelets can take up  $Zn^{2+}$  via so far unknown mechanisms.

The aim of this thesis was to gain insight into the expression of MK and platelet specific  $Zn^{2+}$  transport proteins of the ZIP and ZnT family as a basis to understand  $Zn^{2+}$  homeostasis and  $Zn^{2+}$  dependent signaling in these cells. Using quantitative PCR and *in vitro* differentiated primary MKs, the mRNA expression profile of 24 *Slc30a* and *Slc39a* genes was established in mature MKs, followed by studies addressing the change of mRNA expression during megakaryopoiesis and in response to altered extracellular  $Zn^{2+}$  concentrations.

## 2. Materials and Methods

### 2.1 Materials

#### 2.1.1 Cell culture material

StemPro®-34 serum free medium	Thermo Fisher Scientific (Waltham, USA)
StemPro®-34 nutrient supplement	Thermo Fisher Scientific (Waltham, USA)
Stem cell factor (SCF)	Invitrogen (Carlsbad, USA)
Thrombopoetin (TPO)	Kindly provided by Prof Schulze
ZnCl <sub>2</sub> (10mM stock solution)	Sigma-Aldrich (Taufkirchen, Germany)
TPEN (N,N,N',N'-tetrakis (2-pyridylmethyl)ethylenediamine 100mM stock solution	Tocris (Bristol, UK)
Bovine serum albumin (BSA)	Invitrogen (Carlsbad, USA)
Dulbecco's phosphate buffered saline	Invitrogen (Carlsbad, USA)
22/27G x 1 ½ in. needles	B. Braun (Melsungen, Germany)
Single use 5ml syringe	B. Braun (Melsungen, Germany)
Cell strainer 70/100µm	Greiner Bio-One (Frickenhausen, Germany)
6-well cell culture plates	Sarstedt (Nümbrecht, Germany)
10 cm petri dishes	Sarstedt (Nümbrecht, Germany)
15 mL collection tubes	Sarstedt (Nümbrecht, Germany)

#### 2.1.2 Mouse models

C57BL/6 mice	Janvier (Le Genest-Saint-Isle, France)
--------------	--

### 2.1.3 RNA extraction material

NucleoSpin® RNA II Kit	Macherey-Nagel (Düren, Germany)
Bond-Breaker™ TCEP solution	Thermo Fisher Scientific (Waltham, USA)
Ethanol 99.8%	Honeywell (Charlotte, USA)
Nuclease-free H <sub>2</sub> O	Roth (Karlsruhe, Germany)
1.5 ml reaction tubes nuclease-free	Sarstedt (Nümbrecht, Germany)
15 mL falcon tubes	Greiner Bio-One (Frickenhausen, Germany)

### 2.1.4 cDNA synthesis material

10X RT buffer	Applied Biosystems (Waltham, USA)
25X dNTP mix (100mM)	Applied Biosystems (Waltham, USA)
10X RT random primers	Applied Biosystems (Waltham, USA)
MultiScribe™ reverse transcriptase	Applied Biosystems (Waltham, USA)
0.5 mL reaction tubes nuclease-free	Eppendorf (Hamburg, Germany)

### 2.1.5 Real time polymerase chain reaction material

FastStart Universal SYBR Green Master	Roche (Indianapolis, USA)
384 well Multiply®-PCR plate	Sarstedt (Nümbrecht, Germany)
Adhesive qPCR seal	Sarstedt (Nümbrecht, Germany)

### 2.1.6 RT-PCR primer

All oligonucleotides were ordered from Microsynth (Balgach, Switzerland). Lyophilizate was dissolved in nuclease-free H<sub>2</sub>O to a concentration of 100 µM and stored at -20°C.

Primer name	Sequence	Amplicon Size
mRplp0 Forward	5'-GAAACTGCTGCCTCACATCCG-3'	146 bp
mRplp0 Reverse	5'-CTGGCACAGTGACCTCACACG-3'	
mltga2b Forward	5'-GCCCTTCTTCCATTGCGC-3'	138 bp
mltga2b Reverse	5'-GCTCACACTCCACCACCGTA-3'	
mGp1ba Forward	5'-CTCTGTTCTCCAAAGGACTGTCT-3'	131 bp
mGp1ba Reverse	5'-TCACAGTTTACTTCCAGCAGGC3-3'	
mMcl-1 Forward	5'-GCAGCGCAACCACGAGA-3'	85 bp
mMcl-1 Reverse	5'-TCGAGAAAAAGATTTAACATCGCC-3'	
mBcl2l1 Forward	5'-CGGATTGCAAGTTGGATGG-3'	108 bp
mBcl2l1 Reverse	5'-TGCTGCATTGTTCCCGTAGA-3'	
mZIP1 Forward	5'-ATTCCCGACGCGAGGC-3'	146 bp
mZIP1 Reverse	5'-TCCGATGCGACTGCTTCTG-3'	
mZIP2 Forward	5'-CAG ATG GAT GCA GCT ACA GGTC-3'	82 bp
mZIP2 Reverse	5'-CTG CTC CCA AGA AGA CAC CTG-3'	
mZIP3 Forward	5'-GTCCCTCTGCAACACCTTCG-3'	147 bp
mZIP3 Reverse	5'-ACCATCATGAGCGTCTCCG-3'	
mZIP4 Forward	5'-GGCCTGTAAATACGCTGGTG-3'	136 bp
mZIP4 Reverse	5'-TCTGGACTCCAGGACTGATTCTG-3'	
mZIP5 Forward	5'-TGGGAGATTGCCTGCACA-3'	147 bp
mZIP5 Reverse	5'-CCTGAAGCAGCATGGCAA-3'	
mZIP6 Forward	5'-CACGCCTCGTAAAGGCTTCTC-3'	134 bp
mZIP6 Reverse	5'-ATCTGTGGCCATTGCACCTT-3'	
mZIP7 Forward	5'-GGTTGCGGAAAAGGAGAGG-3'	137 bp
mZIP7 Reverse	5'-AAGTTGTGTGCCAAGTCAGCAG-3'	



mZIP8 Forward	5'-CGGACACATCCACTTCGACA-3'	129 bp
mZIP8 Reverse	5'-AGCGTGATCATCCAGGCAAT-3'	
mZIP9 Forward	5'-GGAGGGCAGAATGGATGACTT-3'	150 bp
mZIP9 Reverse	5'-ACAGAGAAGACCAGCACCCAG-3'	
mZIP10 Forward	5'-GAGCGGAGAGGAGATGCACA-3'	145 bp
mZIP10 Reverse	5'-GGCCATGGTCATGGTCTTCA-3'	
mZIP11 Forward	5'-GGGCACCCTACAGTATCCAGC-3'	150 bp
mZIP11 Reverse	5'-GCTTCCGTCTAAGATCCGCC-3'	
mZIP12 Forward	5'-GCCAGCCTCCAACAGAAATG-3'	142 bp
mZIP12 Reverse	5'-TGTTGTGGTCACTCCTGACTCC-3'	
mZIP13 Forward	5'-CTGCCACCTCTGCCACTG-3'	130 bp
mZIP13 Reverse	5'-GGGAACCTCCAGCCCTTTC-3'	
mZIP14 Forward	5'-CCTGGCTATTGGTGCCTCC-3'	119 bp
mZIP14 Reverse	5'-CAGCATTGAGCAGGATGACG-3'	
mZnT1 Forward	5'-AATTCCAACGGGCTGAAGG-3'	150 bp
mZnT1 Reverse	5'-TCCTCGCATATTCAGCTGCC-3'	
mZnT2 Forward	5'-CCCATCTGCACCTTCCTCTTC-3'	139 bp
mZnT2 Reverse	5'-CCACGGACAGCAGGAGATTT-3'	
mZnT3 Forward	5'-GGAGACCACCCGCCTAGTG-3'	120 bp
mZnT3 Reverse	5'-ATCCCCTCAAGCTTGGGCT-3'	
mZnT4 Forward	5'-ATGCACTCCATATGCTAACTGACC-3'	134 bp
mZnT4 Reverse	5'-ACACTGATCATGGCCGACAA-3'	
mZnT5 Forward	5'-ACCACTAAGGACCTTGCTGCTG-3'	149 bp
mZnT5 Reverse	5'-CGAAAAGCAGTAAGCAGATCACA-3'	
mZnT6 Forward	5'-TGGGAAAGTGCTCCTCCAGAC-3'	131 bp
mZnT6 Reverse	5'-GAGCCAAATCCAAGGGTCC-3'	
mZnT7 Forward	5'-GGCAAGATCTCAGGCTGGTTT-3'	136 bp
mZnT7 Reverse	5'-GATCAAGCCTAGGCAGTTGCTC-3'	
mZnT8 Forward	5'-AGTTGATGGCGTGATCTCCG-3'	130 bp
mZnT8 Reverse	5'-TTGAGCAATTCCTGTCCGC-3'	
mZnT9 Forward	5'-AGGCGCAGAACTCAAAGCTC-3'	150 bp

mZnT9 Reverse	5'-CACTGGACTTAAGGCAGAACTCG-3'	
mZnT10 Forward	5'-GGTGATTCCCTGAACACCGA-3'	139 bp
mZnT10 Reverse	5'-TAGCCGTGATGACCACAACC-3'	

### 2.1.7 Technical equipment

Pipettes 1000/200/10µl	Eppendorf (Hamburg, Germany)
Pipetting tips (sterile, nuclease-free)	Sarstedt (Nümbrecht, Germany)
Biofuge Primo R centrifuge (RNA-extraction and reverse transcription)	Thermo Fisher Scientific (Waltham, USA)
Centrifuge 5810 R (Cell Culture, RT-PCR)	Eppendorf (Hamburg, Germany)
PCR-thermocycler (reverse transcription)	Peqlab (Erlangen, Germany)
ViiA™7 RT-PCR machine	Applied Biosystems (Waltham, USA)
NanoDrop spectrophotometer	Thermo Fisher Scientific (Waltham, USA)

### 2.1.8 Software

Primer Express 3.0	Applied Biosystems (Waltham, USA)
ViiA™7 Software V1.2.1	Applied Biosystems (Waltham, USA)
GraphPad Prism 6	GraphPad Software (San Diego, USA)
Microsoft Excel 2010	Microsoft (Redmond, USA)
Adobe Photoshop CS6	Adobe (Dublin, Ireland)
Primer-BLAST online tool	NCBI (Bethesda, USA)

## **2.2 Methods**

### **2.2.1 Extraction of murine bone marrow cells**

Femurs of freshly killed mice were dissected and bone marrow was flushed into 6-well cell culture plates using 22G x 1½ in. needles and 1mL StemPro-34 medium per mouse. Cells were suspended using a 5 ml syringe with 22G x 1½ in. needles 15 times, then using 27G x 1½ in. needles 3 times. Cells were strained through an 70µm cell strainer into a collection tube afterwards.

### **2.2.2 Culturing of megakaryocytes**

1mL of the bone marrow single cell suspension was pipetted in a 10cm Petri dish and 9mL StemPro-34 was added. Then, 5µl stem cell factor was added and incubated at 37°C and 5% CO<sub>2</sub> for 48h. After 2 days, cell suspension was pipetted into a 15mL collection tube and centrifuged at 200 x g for 5 min. The supernatant was discarded, the cell pellet was resuspended using 10mL StemPro medium. 5µL SCF and 50µL thrombopoetin were added and cells were incubated in a 10cm petri dish for another 48h at 37°C and 5%CO<sub>2</sub>. Afterwards, the cell suspension was again pipetted into a 15mL collection tube and centrifuged at 200 x g for 5 min. The supernatant was discarded, and the cell pellet was resuspended using 10mL StemPro medium.

### **2.2.3 Stimulation of megakaryocytes during megakaryopoiesis**

The cell suspension was pipetted again into a 10 cm Petri dish and 50µL TPO was added. Then, cells were stimulated with different concentrations of ZnCl<sub>2</sub> and TPEN for the experiments and again incubated for another 24h at 37°C and 5% CO<sub>2</sub>.

### **2.2.4 Purification of megakaryocytes**

The cell suspension was pipetted into a 15mL collection tube and centrifuged at 200 x g for 5 min. Supernatant was discarded except the last 1mL, cell pellet was resuspended. To get rid of contamination with smaller cells than megakaryocytes, a BSA/PBS gradient was used. First, a 1.5% bovine serum albumin in phosphate buffered saline solution and a 3.0% BSA/PBS solution were prepared. To set up

the gradient, 1.5mL of 3.0% BSA/PBS was pipetted into a 15mL collection tube. Then, 1.5mL of 1.5%BSA/PBS was carefully pipetted on top. Afterwards, the cell suspension was carefully pipetted on top. Because of their size, megakaryocytes settle down faster in the BSA/PBS gradient than smaller cells. After 30 min, the BSA gradient was carefully sucked away without destroying the megakaryocyte pellet at the bottom of the 15mL falcon. The cells then were stored at -80°C till they were used for RNA extraction or seeded to 6-well plates for the experiment described below.

### **2.2.5 Stimulation of matured megakaryocytes**

For the time-dependent stimulation experiments, the mature megakaryocytes were seeded into 6-well-plates after purification, adding 10µL TPO and 200µM ZnCl<sub>2</sub> respectively 10µM TPEN. At the designated time points of 0h ,1h, 3h, 8h and 24h after stimulation, the cells were collected by centrifuging at 200 x g for 5 min. The supernatant was discarded and the cells were stored at -80°C.

### **2.2.6 Collecting of cells during all stages of megakaryopoiesis**

For the last experiment of this work, cells were collected every 24h during megakaryopoiesis. The first cells were collected directly after extraction from the bone marrow, the second after 24h of treatment with SCF, the third after 48h of SCF treatment, the fourth after another 24h of treatment with SCF and TPO, the next after 48h SCF and another 48h of combined SCF and TPO treatment, and the last two after another 24h respectively 48h of treatment with TPO alone. All cells suspensions were purified using the protocol from chapter 2.2.4 to eliminate the unwanted smaller cells like erythrocytes and small hematopoietic cells. Afterwards, the cells were stored at -80°C.

### **2.2.7 RNA purification**

RNA was purified using the NucleoSpin®RNA II Kit. At first, 350µl RA1 lysis buffer and 8µl BondBreaker® TCEP solution was added to the pellet to lyse the cells. After vortexing and 5 min waiting at room temperature, lysates were filtered using NucleoSpin® filter and centrifugation at 11,000 x g for 1 min. 350µl of 80%

ethanol were added to the flow-through and mixed by pipetting up and down 5 times to precipitate RNA. Lysates were loaded to the NucleoSpin®RNA II column and centrifuged at 11,000 x g for 1 min to bind RNA. The column membrane was desalted using 350µl membrane desalting buffer and centrifuging at 11,000 x g for 1 min. DNA contamination was digested by adding a mixture of 10µl reconstituted rDNAse and 90µl reaction buffer for rDNAse and incubating 15 min at room temperature. For the first washing step, 200µl RA2 Buffer were applied to the column and centrifuged at 11,000 x g for 1 min. The column was placed in a new collection tube afterwards. The second washing step was conducted by adding 600µl RA3 Buffer and centrifuging at 11,000 x g for 1 min. Flow-through was discarded. For the last washing step, 250µl RA3 Buffer were applied and centrifuged at 11,000 x g for 2 min to dry the membrane. Finally, RNA was eluted by adding 20µl nuclease free H<sub>2</sub>O and centrifuging at 11,000 x g for 1 min. RNA was stored at -80°C afterwards.

### **2.2.8 Measurement of RNA concentration**

The RNA concentration was measured by using the NanoDrop 2000 nanospectrophotometer. When concentrations higher than 1000ng/µl were measured, the RNA sample was diluted in nuclease free H<sub>2</sub>O 1:1 and measured again.

### **2.2.9 cDNA synthesis**

RNA samples were diluted in Nuclease-free H<sub>2</sub>O to a total amount of 1µg of RNA and a total volume of 10.5 µL. If the RNA concentration had been too low, the RNA was not diluted. Reverse transcription was performed according to the following protocol:

10X RT buffer	2.0 µL
25X dNTP mix (100mM)	0.8 µL
10X RT random primers	2.0 µL
MultiScribe™ reverse transcriptase	0.5 µL

Nuclease free H <sub>2</sub> O	4.2 µL
RNA sample (total of 1µg RNA)	10.5 µL
Total	20µL

First, the mastermix containing 10X RT buffer, 25X dNTP mix, 10X random Primers, MultiScribe™ reverse transcriptase and nuclease free H<sub>2</sub>O were mixed in a separate 1.5 mL reaction tube. Then the mastermix was added to the RNA sample in a 0.5 mL PCR-tube and put into the thermocycler with this program:

Temperature	Time
25°C	10:00 min
37°C	120:00 min
85°C	05:00 min
4°C	∞ min

### 2.2.10 Primer design

Primers for RT-PCR were designed using the ensembl.org database, the NCBI Primer Blast website and the Primer Express 3.0 Software. Afterwards, primers were tested for correct performance by RT-PCR with mouse cDNA samples from different tissues at descending concentrations. The primer test is presented exemplarily in the appendix; the complete data can be requested from the author.

### 2.2.11 Real time polymerase chain reaction (RT-PCR)

PCR is a common biochemical method to detect specific DNA fragments. The basic principle is the exponential amplification mechanism called replication, naturally taking place during every cell cycle. This mechanism has been adapted to *in vitro* conditions:

First, the double-stranded DNA is split into two single strands through heating to 95°C. Especially smaller DNA fragments like cDNA are split effectively at this temperature. Second, the individually designed primers for the requested sequence are attached to the corresponding DNA sequence. The last step is

conducted by the enzyme DNA-Polymerase, which, starting from the primer, synthesizes the complementary strand. Then, the cycle starts again, exponentially multiplying the requested DNA sequence.

Real time polymerase chain reaction is a special PCR method that allows to determine the amount of DNA copies of a certain sequence in a sample. For this, a fluorescent dye called SYBR® Green is used. It attaches to the double stranded DNA amplicons during the polymerization cycles. When SYBR® Green is attached to double stranded DNA, its fluorescence signal is strongly enhanced. The fluorescence intensity can be measured, and the amount of DNA can be determined. However, the dye unspecifically binds to all double stranded DNA, not only to the requested copies. To make sure that the fluorescence signal is not the signal of nonsense copies which were unintentionally multiplied as well, the product is heated and the melting temperature where the double stranded DNA breaks into single strands is recorded. If the product is free from nonsense copies, only one melting peak should appear. In this case, one can assume that the measured fluorescence amplification originates from the requested DNA sequence.

For the analysis of qPCR data, the measured values for the target gene were normalized to a housekeeping gene to eliminate differences in the total amount of cDNA of the different samples. In this study, for all experiments with megakaryocytes the housekeeping gene ribosomal protein large subunit P0 was used. This gene showed the best performance among the tested housekeeping genes (data not shown) in terms of low standard error and high, stable expression in this cell type. After normalization, the results were analyzed using the comparative CT ( $\Delta\Delta\text{CT}$ ) method to determine gene expression in the experiments of this study.

All primer stock solutions were diluted 1:20 for the RT-PCR, only the mRplp0 forward and reverse primers were diluted 1:10 in nuclease free H<sub>2</sub>O. RT-PCR was then conducted according to the following protocol:

H <sub>2</sub> O	3.5µl
FastStart Universal SYBR Green Master	5µl
Forward primer dilution	0.5µl
Reverse primer dilution	0.5µl
cDNA sample	1µl
Total	10µl

H<sub>2</sub>O, FastStart Universal SYBR Green Master, forward primer and reverse primer were mixed thoroughly in a separate 1.5 mL reaction tube and pipetted onto the 384 well Multiply®-PCR Plate. Afterwards, the cDNA sample was added and the 384 well plate was sealed with the adhesive qPCR seal. Then, the plate was centrifuged at 900 x g for 1 min to eliminate bubbles.

RT-PCR Program:

Temperature	Time	Number of cycles
50°C	02:00 Min	1 cycle
95°C	10:00 Min	1 cycle
95°C	00:10 Min	40 cycles
60°C	00:30 Min	40 cycles
95°C	00:15 Min	1 cycle
60°C	01:00 Min	1 cycle
Heat to 95°C (0.05°C/s)	11:40 Min	1 cycle

### 2.2.12 Statistical methods

Graph Pad Prism 6 was used for statistical analysis. When values were compared to the reference column, one sample t-tests were performed. Two-tailed t-tests were used if two time points except from the reference (day 5) were compared in the megakaryopoiesis experiment (see chapter 2.2.6)



### 3. Results

#### 3.1 *In vitro* cultivation of primary mouse megakaryocytes

Megakaryopoiesis of MKs, that were differentiated from hematopoietic stem cells isolated from bone marrow (BM), was followed up for several days. BM cells were cultured in the presence of stem cell factor (day 1-2), followed by a combination with thrombopoetin (day 3-4) and with TPO alone (day 5 -6). Differentiated MKs were observed on day 5 and 6 (Fig. 4A).

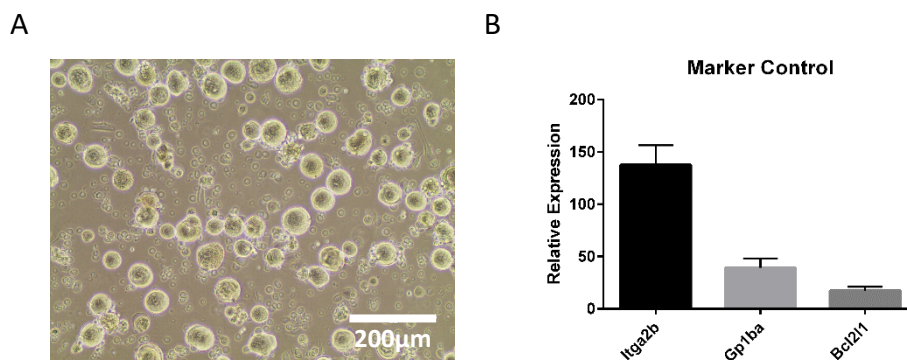


**Figure 4. Characterization of cultivated murine megakaryocytes.** (A) Transmission microscopic image of primary mouse MKs after purification with BSA gradient. (B) mRNA expression of MK specific markers (*Itga2b*; *Gp1ba*) and survival marker (*Bcl2l1*) in mouse MKs at day 5. The housekeeping gene of ribosomal protein large subunit P0 (*Rplp0*) was used as control and set to 100. (n ≥ 3; values: mean + SEM)

The average size of MKs was approximately 50 μm. MK-specific markers like *Itga2b* (ItgαIIb, CD41) and *Gp1ba* (GPIbα, CD42b) were highly expressed, indicating an efficient bone marrow cells differentiation to MKs in this experimental condition. Survival marker *Bcl2l1* was used to monitor cell death which is expressed 5.8-fold lower than *Rplp0* (Fig. 4B).

#### 3.1.2 Cellular Zn<sup>2+</sup> toxicity in primary mouse megakaryocytes

Bone marrow cells were cultured for 5 days to obtain mature MKs. After MK isolation with BSA gradient at day 5, MKs were again cultured in the presence or absence of different concentrations of ZnCl<sub>2</sub> (0; 50; 200; 500 μM) for 24 hours. When cells were treated with 500 μM ZnCl<sub>2</sub>, all MKs died within the observation period (data not shown). In contrast, MKs could survive at lower concentrations

of  $ZnCl_2$  (50  $\mu M$ ) and surprisingly even tolerate 200  $\mu M$  without observation of any obvious cell death (Fig. 5A).

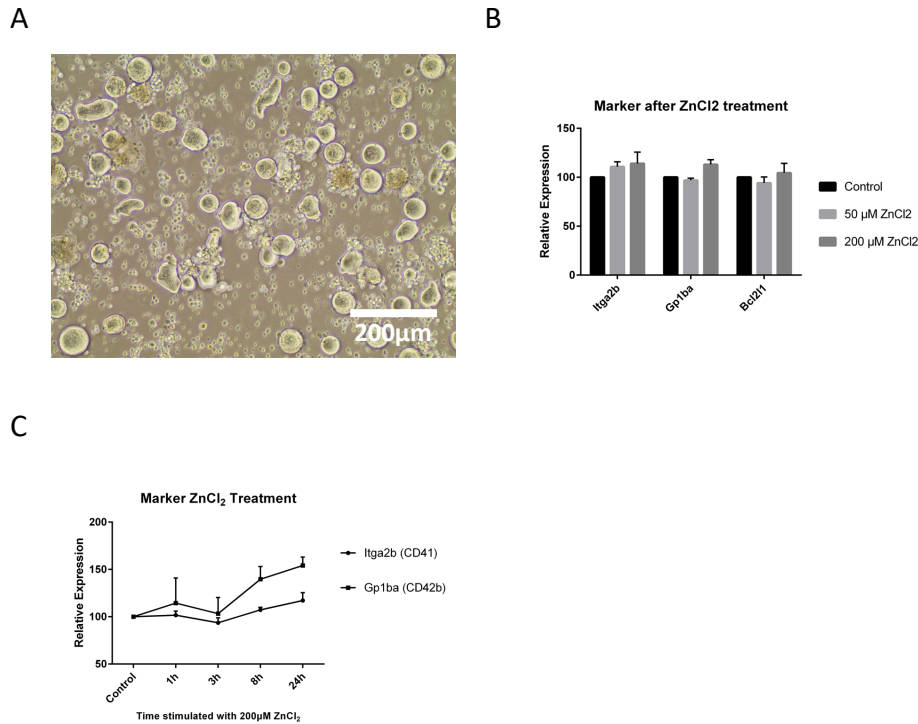


**Figure 5. Effects of extracellular  $ZnCl_2$  in megakaryocytes.** (A) Transmission microscopic image of mature megakaryocytes treated with 200  $\mu M$   $ZnCl_2$  after purification with BSA gradient. (B) mRNA expression of  $ZnCl_2$  treated MKs. Control normalized to *Rplp0* was set to 100. (C) Relative mRNA expression of *Gp1ba* and *Itga2b* in MKs was followed during the indicated time period. MKs were treated with 200  $\mu M$   $ZnCl_2$ . Control normalized to *Rplp0* was set to 100. ( $n \geq 3$  for every experiment, values: mean  $\pm$  SEM)

Expression level of the MK specific marker *Itga2b* slightly increased in a dose dependent manner (50  $\mu M$   $ZnCl_2$ : 11%,  $p=0.16$ ; 200  $\mu M$   $ZnCl_2$ : 14 %,  $p=0.35$ ) when compared to the untreated control MKs, although this change was not statistically significant (Fig. 5B). mRNA expression of *Gp1ba* did not change at 50  $\mu M$   $ZnCl_2$ , but slightly increased at 200  $\mu M$   $ZnCl_2$  (13%,  $p=0.12$ ). Expression of the survival marker *Bcl2l1* did not change under these conditions, excluding  $Zn^{2+}$  toxicity in this condition (Fig. 5B). In the time dependent experiment with mature MKs (Fig. 5C), the *Gp1ba* expression even increased by 54% at time point of 24h ( $p<0.05$ ). Altogether, these results suggest that MKs can tolerate high doses of  $Zn^{2+}$  supplementation for a short time period, although this

treatment seems to rapidly change the expression profile of several genes, including *Gp1ba*.

### 3.1.3 Zn<sup>2+</sup> chelator TPEN inhibits megakaryopoiesis

High concentrations of TPEN (10 μM – 50 μM) are regularly used in mammalian cells to induce experimental Zn<sup>2+</sup> deficiency under *in vitro* conditions. In the presence of low dose of TPEN (1-2 μM), MKs died at day 5 after 24h treatment with TPEN, indicating that late steps of MK maturation are strongly Zn<sup>2+</sup>-dependent. (Fig 6A/B).

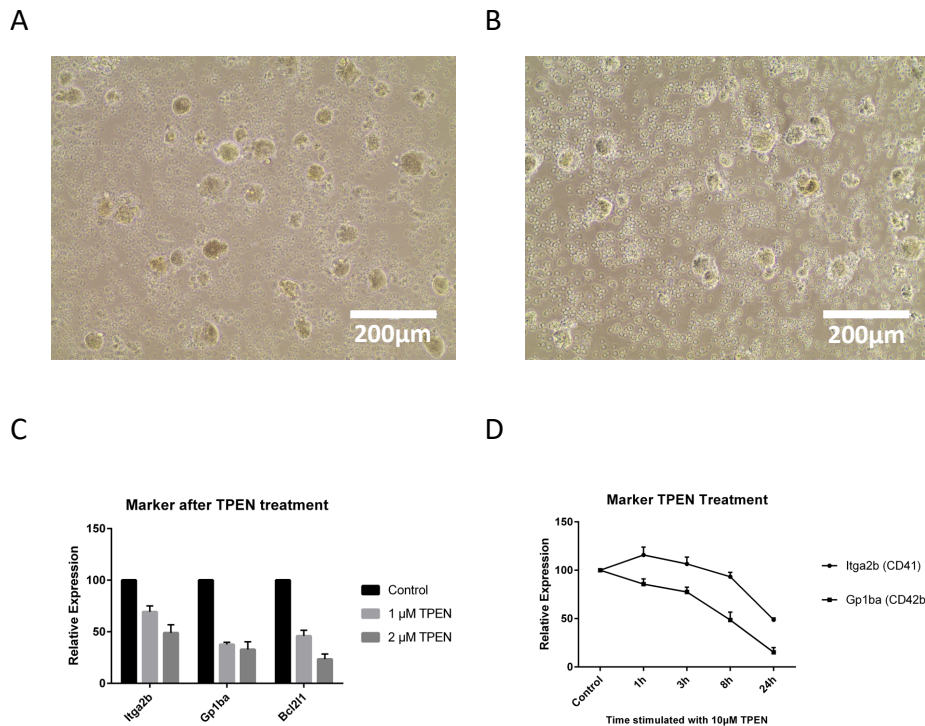


**Figure 6. Zinc chelation reduces survival rate of primary mouse megakaryocytes.**

Transmission microscopic images of mature megakaryocytes treated with 1 μM TPEN (A) and 2μM TPEN (B) after purification with BSA gradient. (C) mRNA expression of TPEN treated MKs. Control normalized to *Rplp0* was set to 100. (D) Relative mRNA expression of *Gp1ba* and *Itga2b* in MKs was followed during the indicated time period. MKs were treated with 10μM TPEN. Control normalized to *Rplp0* was set to 100. (n≥ 3 for every experiment, values: mean ± SEM)

The expression of the MK marker *Itga2b* decreased by 1.4-fold (p<0.05) after treatment with 1 μM TPEN and further decreased after treatment with 2 μM TPEN

(2.0-fold,  $p < 0.05$ ). *Gp1ba* expression decreased by 2.7 or 3.0-fold ( $p < 0.05$ ) when treated with 1  $\mu$ M or 2  $\mu$ M TPEN, respectively. Expression of the survival marker *Bcl2l1* decreased by 2.2 or 4.3-fold ( $p < 0.05$ ) when treated with 1  $\mu$ M or 2  $\mu$ M TPEN (Fig. 6C).

Next, mature MKs were isolated at day 5 and 10  $\mu$ M TPEN was added. *Itga2b* and *Gp1ba* expression was followed for 24 hours. In line with the previous experiment, MK markers strongly decreased within 24 hours. *Itga2b* expression decreased by 2.0-fold; *Gp1ba* expression decreased by 6.6-fold, ( $p < 0.05$ ) indicating a severe toxicity of TPEN treatment in mature MKs (Fig. 6D).

### 3.2 Expression profile of Slc39a genes in mature megakaryocytes

The ZIP protein family (genes: *Slc39a*) has 14 members regulating Zn<sup>2+</sup> influx into mammalian cells. The molecular composition of the Zn<sup>2+</sup> transport machinery is entirely unknown for MKs, therefore quantitative (q) reverse transcriptase (RT)-PCR was performed using mRNAs isolated from bone marrow derived primary murine MKs at day 5. The expression profile of *Slc39a* genes was determined (Fig. 7); relative expression was compared to the expression of the housekeeping gene *Rplp0* which was set to 100.

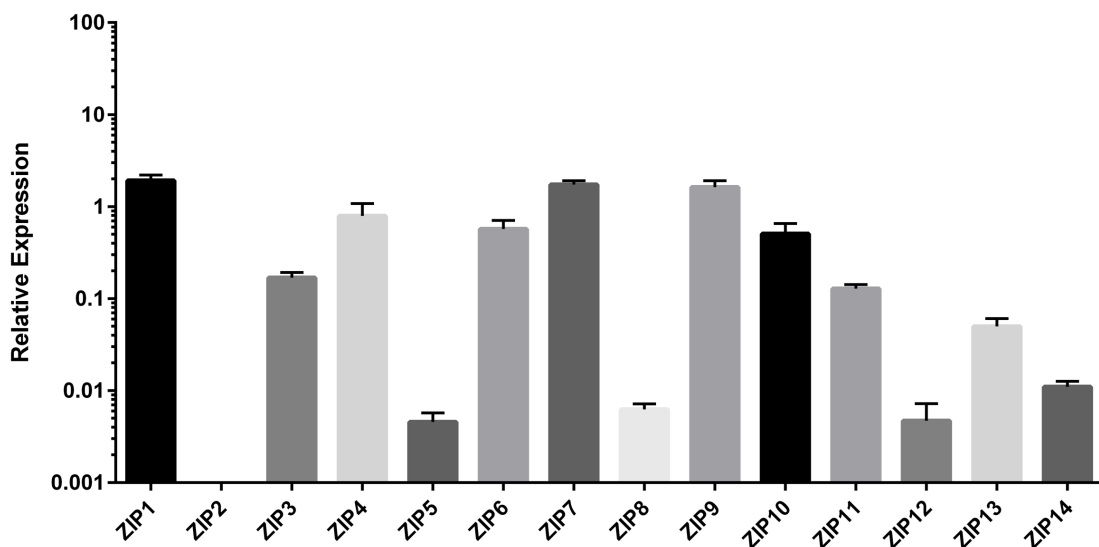


**Figure 7. Relative mRNA expression as determined by C<sub>T</sub> values of *Slc39a* genes encoding ZIP transporters.** mRNA expression profile of mature MKs at day 5 relative to the mRNA level of *Rplp0*, whose expression was set to 100. Bar graphs are shown in logarithmic scale. (n ≥ 3 for every experiment, values: mean + SEM)

ZIP1 was the most abundant Zn<sup>2+</sup> transporter (1.9 % of *Rplp0* expression) compared to other *Slc39a* family members. In contrast, ZIP2 was not detected in MKs using two independent experiments performed with different primer pairs. Based on the mRNA levels for ZIP1 (*Slc39a1*), three different groups of ZIP isoforms were classified: (i) highly abundant expression (threshold: 1.5-fold lower than ZIP1) (ii) moderately (threshold: 15-fold lower than ZIP1), or (iii) the mRNA levels were low or extremely low.

ZIP7 (*Slc39a7*) and ZIP 9 (*Slc39a9*) expression were compared to ZIP1 and found to be nearly similar (ZIP7: 1.1-fold lower, ZIP9: 1.2-fold lower). ZIP4

(*Slc39a4*), ZIP6 (*Slc39a6*) and ZIP10 (*Slc39a10*) expression were significantly lower than ZIP1, but these isoforms were moderately expressed, between 2.4 – 3.8-fold less compared to ZIP1. Abundance of other isoforms were low or extremely low, compared to ZIP1: ZIP3 (*Slc39a3*) and ZIP11 (*Slc39a11*) expression were approximately 11- to 15-fold lower than ZIP1 expression whereas ZIP13 (*Slc39a13*) level was 38-fold lower than ZIP1. Expression of ZIP5 (*Slc39a5*), ZIP8 (*Slc39a8*), ZIP 14 (*Slc39a14*) and ZIP12 (*Slc39a12*) were extremely low, between 170 -400-fold lower than ZIP1.

Isoforms	Relative expression to ZIP1 (fold)	Classification
ZIP2	not detectable	iii
ZIP3	↓ 11	iii
ZIP4	↓ 2.4	ii
ZIP5	↓ 400	iii
ZIP6	↓ 3.4	ii
ZIP7	↓ 1.1	i
ZIP8	↓ 300	iii
ZIP9	↓ 1.2	i
ZIP10	↓ 3.8	ii
ZIP11	↓ 15	ii
ZIP12	↓ 400	iii
ZIP13	↓ 38	iii
ZIP14	↓ 170	iii

**Table 1. Relative expression of ZIPs.** ZIP1 (*Slc39a1*) compared to other ZIP isoforms.

### 3.2.1 Regulation of *Slc39a1* (ZIP1)

To follow Zn<sup>2+</sup> dependent regulation of *Slc39a* (ZIP) family members, this study focuses on the analysis of genes which are highly or moderately expressed in mature MKs. Although mRNA levels of ZIP1 were found to be the highest of all ZIPs in mouse MKs, extracellular ZnCl<sub>2</sub> in concentrations of 50 μM and 200 μM did not influence mRNA expression of this gene in mature MKs (Fig. 8A, B) However, treatment with TPEN, inducing intracellular Zn<sup>2+</sup> deficit, led to rapid inhibition of *Slc39a1* mRNA expression.

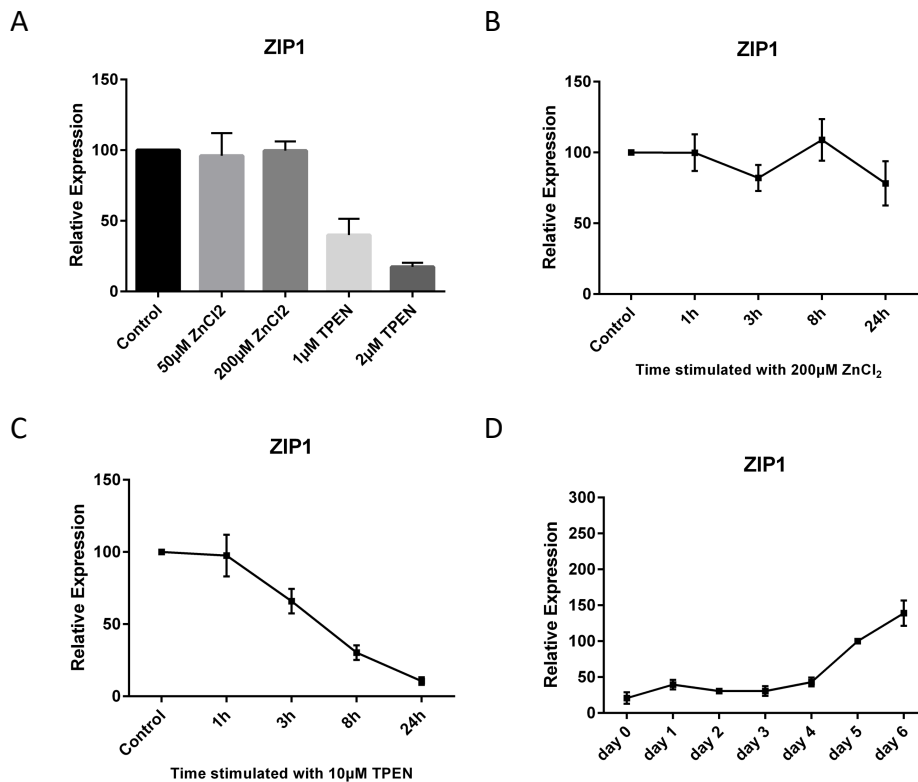


**Figure 8. Relative mRNA expression of *Slc39a1* (ZIP1) in mouse MKs.** (A) Relative mRNA expression of ZIP1 in mature primary MKs after 24h stimulation with different concentration of ZnCl<sub>2</sub> or TPEN. Control normalized to *Rplp0* was set to 100. (B) Relative mRNA expression of ZIP1 in mature MKs was followed at different time points (0, 1, 3, 8, 24 hours) in the presence of extracellular ZnCl<sub>2</sub> (200 µM) or (C) in the presence of TPEN (10 µM). Untreated control (0) normalized to *Rplp0* was set to 100. (D) Relative mRNA expression of ZIP1 was followed and stimulated with SCF (day 0 – 2), SCF/TPO (day 3 – 4) and TPO (day 5 - 6) during megakaryopoiesis. Day 5 values normalized to *Rplp0* were set to 100 (n ≥ 3, values: mean ± SEM).

Dose dependent inhibition was found in the presence of 1 (2.5-fold, p<0.05) or 2 µM TPEN (5.8-fold, p<0.05) after 24h of treatment (Fig. 8A). Treatment of MKs with 10µM TPEN (Fig. 8C) strongly inhibits mRNA expression of *Slc39a1* after 24h by 9.5-fold (p<0.05). *Slc39a1* mRNA expression was weakly detected in bone marrow derived hematopoietic cells or precursors of MKs from day 0 until day 3, but it is strongly upregulated during MK differentiation between day 3 and day 6 (4.5-fold, p<0.05), when cells were treated only with TPO (Fig. 8D).

### 3.2.2 Regulation of *Slc39a3* (ZIP3)

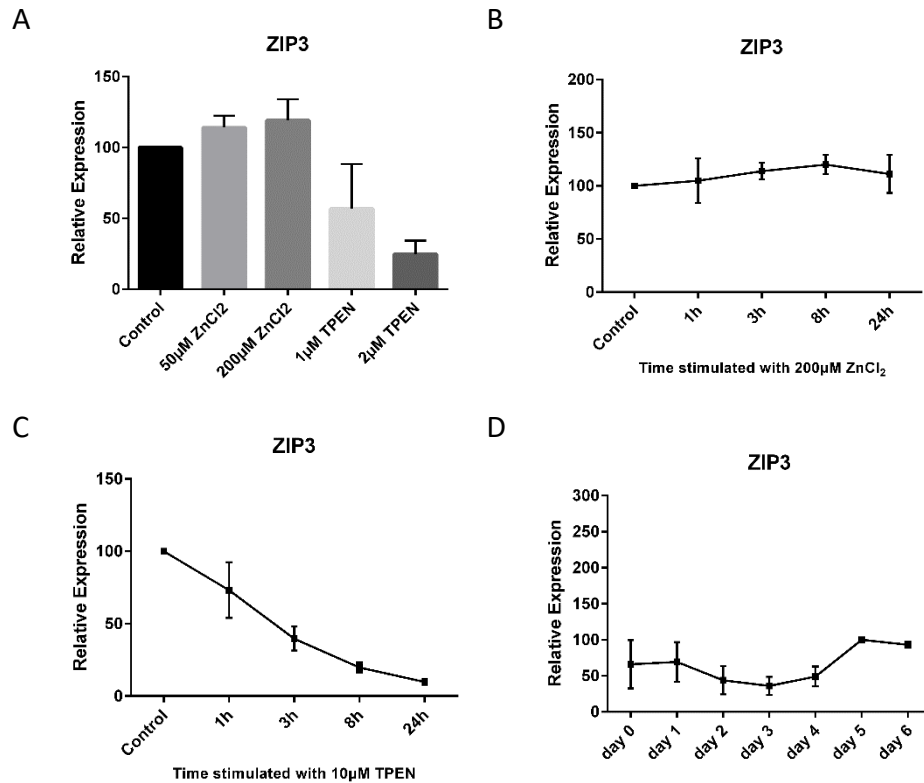


**Figure 9. Relative mRNA expression of *Slc39a3* (ZIP3) in mouse MKs. (A)** Relative mRNA expression of ZIP3 in mature primary MKs after 24h stimulation with different concentration of ZnCl<sub>2</sub> or TPEN. Control normalized to *Rplp0* was set to 100. **(B)** Relative mRNA expression of ZIP3 in mature MKs was followed at different time points (0, 1, 3, 8, 24 hours) in the presence of extracellular ZnCl<sub>2</sub> (200 μM) or **(C)** in the presence of TPEN (10 μM). Untreated control (0) normalized to *Rplp0* was set to 100. **(D)** Relative mRNA expression of ZIP3 was followed and stimulated with SCF (day 0 – 2), SCF/TPO (day 3 – 4) and TPO (day 5 - 6) during megakaryopoiesis. Day 5 values normalized to *Rplp0* were set to 100 (n ≥ 3, values: mean ± SEM).

ZIP3 is a moderately expressed ZIP family member in mouse MKs. Zn<sup>2+</sup> supplementation did not change mRNA expression of *Slc39a3*. After treatment with TPEN, dose dependent changes were detected by 4-fold (p<0.05) in the presence of 2 μM TPEN (Fig. 9A). Zn<sup>2+</sup>-supplementation did not change the mRNA levels of *Slc39a3* (Fig. 9B). After incubation of MKs with 10μM TPEN (Fig. 9C), mRNA levels strongly decreased by 10.2-fold within 24 hours (p<0.05). During megakaryopoiesis, expression levels of *Slc39a3* slightly increased between day 3 and 6 (2.6-fold, p<0.05) when TPO was presented in the medium (Fig. 9D).



### 3.2.3 Regulation of *Slc39a4* (ZIP4)

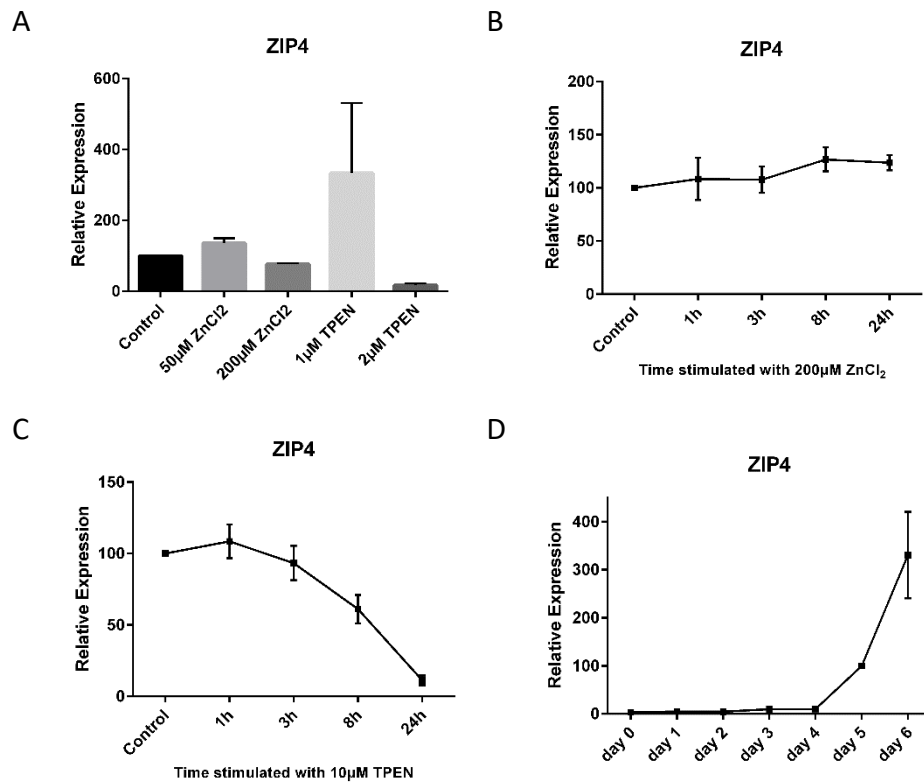


**Figure 10. Relative mRNA expression of *Slc39a4* (ZIP4) in mouse MKs.** (A) Relative mRNA expression of ZIP4 in mature primary MKs after 24h stimulation with different concentration of ZnCl<sub>2</sub> or TPEN. Control normalized to *Rplp0* was set to 100. (B) Relative mRNA expression of ZIP4 in mature MKs was followed at different time points (0, 1, 3, 8, 24 hours) in the presence of extracellular ZnCl<sub>2</sub> (200 μM) or (C) in the presence of TPEN (10 μM). Untreated control (0) normalized to *Rplp0* was set to 100. (D) Relative mRNA expression of ZIP4 was followed and stimulated with SCF (day 0 – 2), SCF/TPO (day 3 – 4) and TPO (day 5 - 6) during megakaryopoiesis. Day 5 values normalized to *Rplp0* were set to 100 (n ≥ 3, values: mean ± SEM).

*Slc39a4* mRNA is moderately expressed and no significant change was observed during 50μM Zn<sup>2+</sup> supplementation. However, a slight but significant downregulation by 24% (p<0.05) was observed in the presence of 200 μM ZnCl<sub>2</sub> (Fig. 10A), and this effect was not obvious using mature MKs (Fig. 10B). Interestingly, when cells were treated with 1μM TPEN, ZIP4 expression was increased by 2.4-fold. However, it was not significant because of the variability of the results (p=0.32). When treated with 2μM TPEN, mRNA level of *Slc39a4* was decreased by 3.8-fold (p<0.05) and 8.9-fold (p<0.05) decrease was observed when cells were treated with 10μM TPEN for 24 hours. Importantly, *Slc39a4*

mRNA expression was very low during BM cell differentiation, but it was strongly upregulated only in the presence of TPO between day 4 and day 6 (31.9-fold,  $p < 0.05$ ).

### 3.2.4 Regulation of *Slc39a6* (ZIP6)

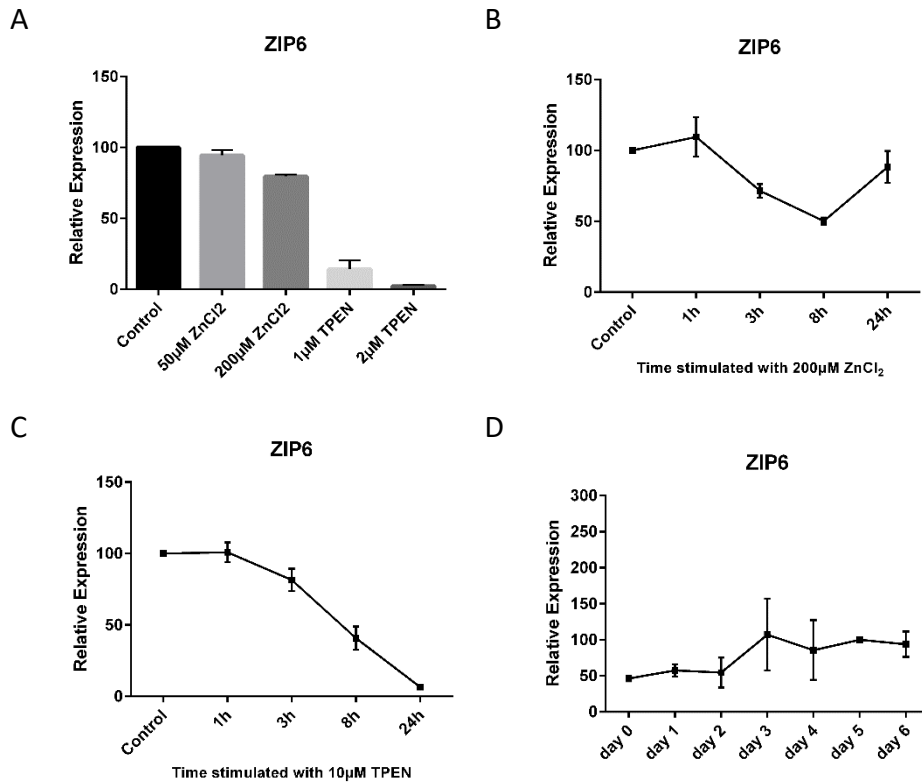


**Figure 11. Relative mRNA expression of *Slc39a6* (ZIP6) in mouse MKs.** (A) Relative mRNA expression of ZIP6 in mature primary MKs after 24h stimulation with different concentration of ZnCl<sub>2</sub> or TPEN. Control normalized to *Rplp0* was set to 100. (B) Relative mRNA expression of ZIP6 in mature MKs was followed at different time points (0, 1, 3, 8, 24 hours) in the presence of extracellular ZnCl<sub>2</sub> (200 μM) or (C) in the presence of TPEN (10 μM). Untreated control (0) normalized to *Rplp0* was set to 100. (D) Relative mRNA expression of ZIP6 was followed and stimulated with SCF (day 0 – 2), SCF/TPO (day 3 – 4) and TPO (day 5 - 6) during megakaryopoiesis. Day 5 values normalized to *Rplp0* were set to 100 ( $n \geq 3$ , values: mean  $\pm$  SEM).

ZIP6 is a moderately expressed ZIP family member. Under Zn<sup>2+</sup> supplementation, 50 μM ZnCl<sub>2</sub> did not lead to significant changes of mRNA expression. However, 200 μM ZnCl<sub>2</sub> treatment (Fig. 11A) slightly decreased the level of *Slc39a6* by 20.4% ( $p < 0.05$ ). When the effects of Zn<sup>2+</sup> supplementation were observed for 24 hours (Fig. 11B), mRNA level of ZIP6 interestingly dropped

down after 8 hours to 50% ( $p < 0.05$ ) and slightly increased again afterwards. TPEN treatment (Fig. 11A) strongly decreased the mRNA levels in both conditions (1  $\mu$ M TPEN: 7.1-fold; 2  $\mu$ M TPEN: 43-fold,  $p < 0.05$ ). When cells were treated with 10  $\mu$ M TPEN (Fig. 11C), expression again decreased by 15.2-fold ( $p < 0.05$ ). Significant changes in expression of ZIP6 between day 0 and day 6 of megakaryopoiesis were not detected (Fig. 11D).

### 3.2.5 Regulation of *Slc39a7* (ZIP7)

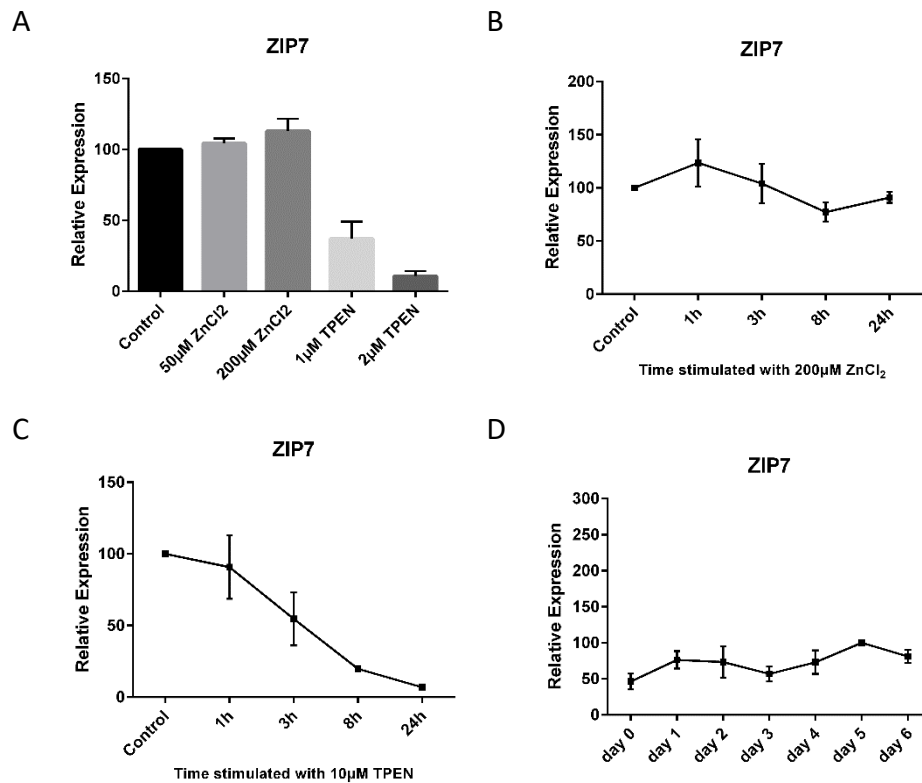


**Figure 12. Relative mRNA expression of *Slc39a7* (ZIP7) in mouse MKs.** (A) Relative mRNA expression of ZIP7 in mature primary MKs after 24h stimulation with different concentration of ZnCl<sub>2</sub> or TPEN. Control normalized to *Rplp0* was set to 100. (B) Relative mRNA expression of ZIP7 in mature MKs was followed at different time points (0, 1, 3, 8, 24 hours) in the presence of extracellular ZnCl<sub>2</sub> (200  $\mu$ M) or (C) in the presence of TPEN (10  $\mu$ M). Untreated control (0) normalized to *Rplp0* was set to 100. (D) Relative mRNA expression of ZIP7 was followed and stimulated with SCF (day 0 – 2), SCF/TPO (day 3 – 4) and TPO (day 5 - 6) during megakaryopoiesis. Day 5 values normalized to *Rplp0* were set to 100 ( $n \geq 3$ , values: mean  $\pm$  SEM).

ZIP7 is one of the dominantly expressed ZIP family members in murine primary megakaryocytes. Treatment of cells with 50  $\mu$ M ZnCl<sub>2</sub> or 200  $\mu$ M ZnCl<sub>2</sub> did not

lead to significant changes in mRNA expression level of *Slc39a7* (Fig. 12A). However, when cells were treated with TPEN, mRNA expression moderately or strongly decreases (1  $\mu$ M TPEN: 2.7-fold; 2 $\mu$ M TPEN: 9.2-fold,  $p < 0.05$ ). Zn<sup>2+</sup> supplementation with 200 $\mu$ M ZnCl<sub>2</sub> treatment showed no significant change in expression levels in mature MKs during the observation period (Fig. 12B). However, 10 $\mu$ M TPEN (Fig. 12C) strongly decreased the *Slc39a7* mRNA level in mature MKs (14.4-fold after 24h). During megakaryopoiesis, no significant change in mRNA expression of *Slc39a7* was observed between day 0 and day 6 (Fig. 12D).

### 3.2.6 Regulation of *Slc39a9* (ZIP9)

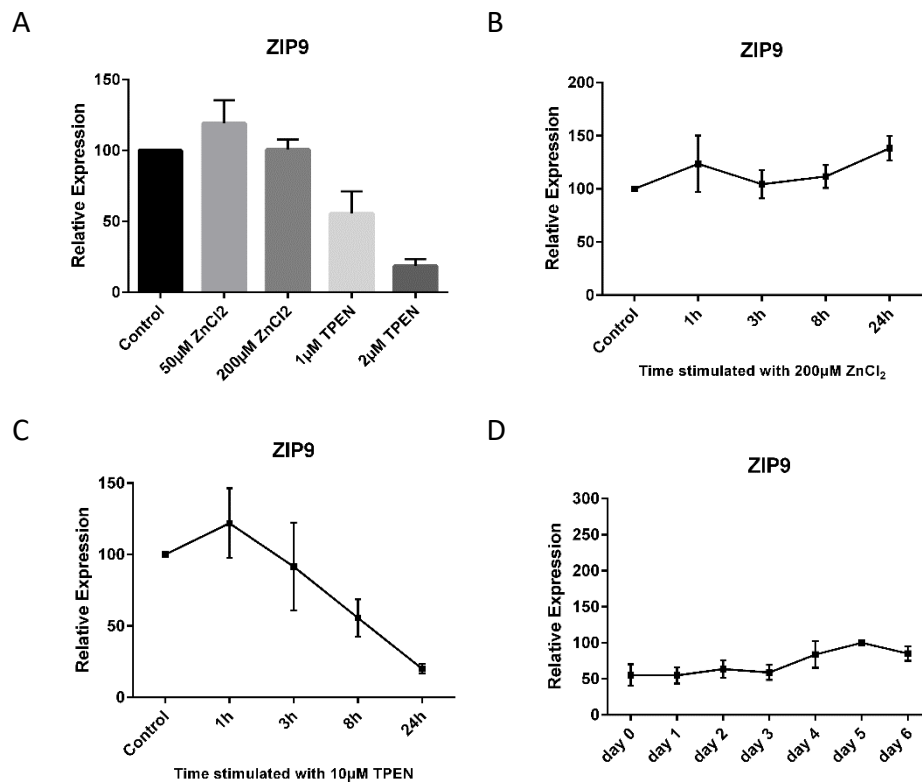


**Figure 13. Relative mRNA expression of *Slc39a9* (ZIP9) in mouse MKs.** (A) Relative mRNA expression of ZIP9 in mature primary MKs after 24h stimulation with different concentration of ZnCl<sub>2</sub> or TPEN. Control normalized to *Rplp0* was set to 100. (B) Relative mRNA expression of ZIP9 in mature MKs was followed at different time points (0, 1, 3, 8, 24 hours) in the presence of extracellular ZnCl<sub>2</sub> (200  $\mu$ M) or (C) in the presence of TPEN (10  $\mu$ M). Untreated control (0) normalized to *Rplp0* was set to 100. (D) Relative mRNA expression of ZIP9 was followed and stimulated with SCF (day 0 – 2), SCF/TPO (day 3 – 4) and TPO (day 5 - 6) during

megakaryopoiesis. Day 5 values normalized to *Rplp0* were set to 100 ( $n \geq 3$ , values: mean  $\pm$  SEM).

ZIP9 is the third-abundant ZIP transporter in murine primary megakaryocytes.  $Zn^{2+}$  supplementation by 50  $\mu M$   $ZnCl_2$  or 200  $\mu M$   $ZnCl_2$  did not alter mRNA expression of *Slc39a9* (Fig. 13 A, B). When MKs were treated with 1  $\mu M$  TPEN, *Slc39a9* expression was found to be decreased by 1.8-fold ( $p=0.066$ ). Stimulation of cells with 2  $\mu M$  TPEN lead to 5.4-fold decrease in mRNA expression ( $p<0.05$ ). When cells were stimulated with 10  $\mu M$  TPEN (Fig. 13C), *Slc39a9* mRNA expression level decreased significantly by 5-fold after 24h ( $p<0.05$ ). It was not possible to observe any change during bone marrow cell differentiation and megakaryocyte maturation (Fig. 10D).

### **3.2.7 Regulation of *Slc39a10* (ZIP10)**

ZIP10 appears to be moderately expressed in murine primary MKs. Treatment with 50  $\mu M$   $ZnCl_2$  did not change *Slc39a10* mRNA expression level significantly. However, when the MKs were treated with the higher dose, *Slc39a10* expression decreased by 2.8-fold ( $p<0.05$ ), indicating an important role of  $Zn^{2+}$  in the gene regulation of *Slc39a10*. Stimulation of cells with 2  $\mu M$  TPEN lead to downregulation of gene expression by 53-fold ( $p<0.05$ ) though (Fig. 14A). Again, treatment of matured MKs for 24 hours with 200  $\mu M$   $ZnCl_2$  lead to downregulation of this isoform by 3.2-fold after 3 hours ( $p<0.05$ ) and cells kept this low mRNA level at later time points (Fig. 14 B). Treatment of cells with 10  $\mu M$  TPEN (Fig.14C) lead to 40.5-fold downregulation of *Slc39a10* mRNAs after 24h ( $p<0.05$ ). Interestingly, during bone marrow cell differentiation, no significant change in mRNA expression was detected (Fig. 14D).

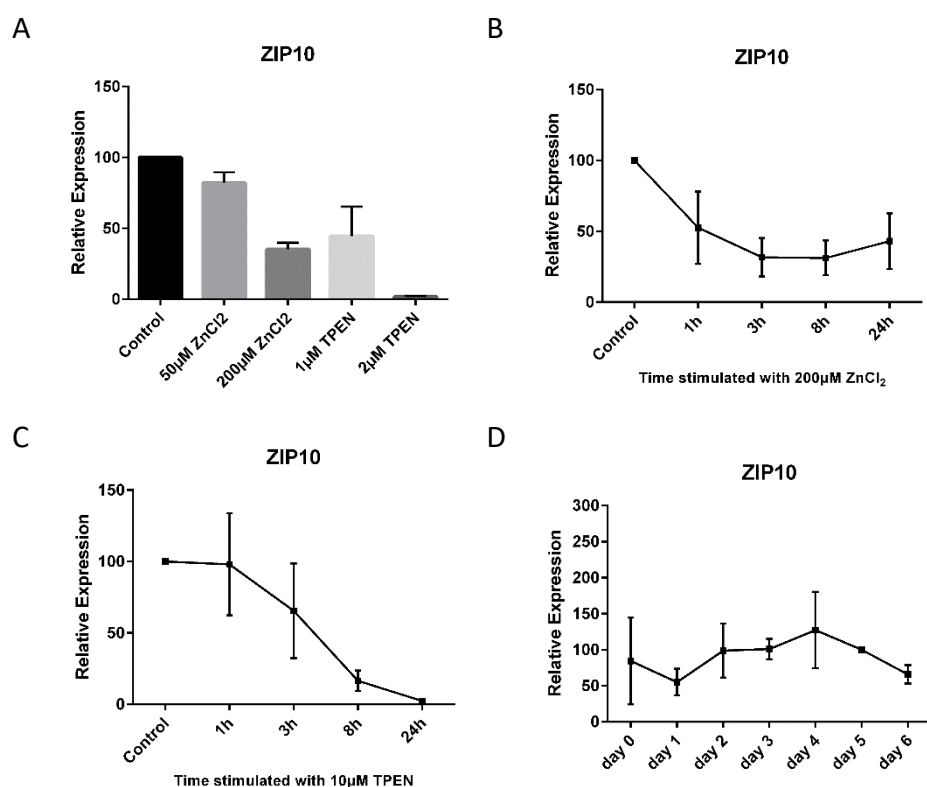


**Figure 14. Relative mRNA expression of *Slc39a10* (ZIP10) in mouse MKs.** (A) Relative mRNA expression of ZIP10 in mature primary MKs after 24h stimulation with different concentration of ZnCl<sub>2</sub> or TPEN. Control normalized to *Rplp0* was set to 100. (B) Relative mRNA expression of ZIP10 in mature MKs was followed at different time points (0, 1, 3, 8, 24 hours) in the presence of extracellular ZnCl<sub>2</sub> (200 μM) or (C) in the presence of TPEN (10 μM). Untreated control (0) normalized to *Rplp0* was set to 100. (D) Relative mRNA expression of ZIP10 was followed and stimulated with SCF (day 0 – 2), SCF/TPO (day 3 – 4) and TPO (day 5 - 6) during megakaryopoiesis. Day 5 values normalized to *Rplp0* were set to 100 (n ≥ 3, values: mean ± SEM).

### 3.2.8 Regulation of *Slc39a11* (ZIP11)

ZIP11 appears to be moderately expressed in murine MKs. Zinc supplementation was sufficient to change the mRNA levels, a slight increase by 20% was observed (p < 0.05). TPEN treatment strongly reduces the mRNA levels of *Slc39a11* (1 μM: 16-fold; 2 μM: 48-fold, p < 0.05) (Fig. 15A). 200 μM ZnCl<sub>2</sub> did not induce significant changes in *Slc39a11* expression in mature MKs during 24h (Fig. 15B), but 10 μM TPEN treatment resulted in a strong decrease of mRNA levels by 23.8-fold (p < 0.05) (Fig. 15C). During megakaryopoiesis, no significant change of expression was measured (Fig. 15D).

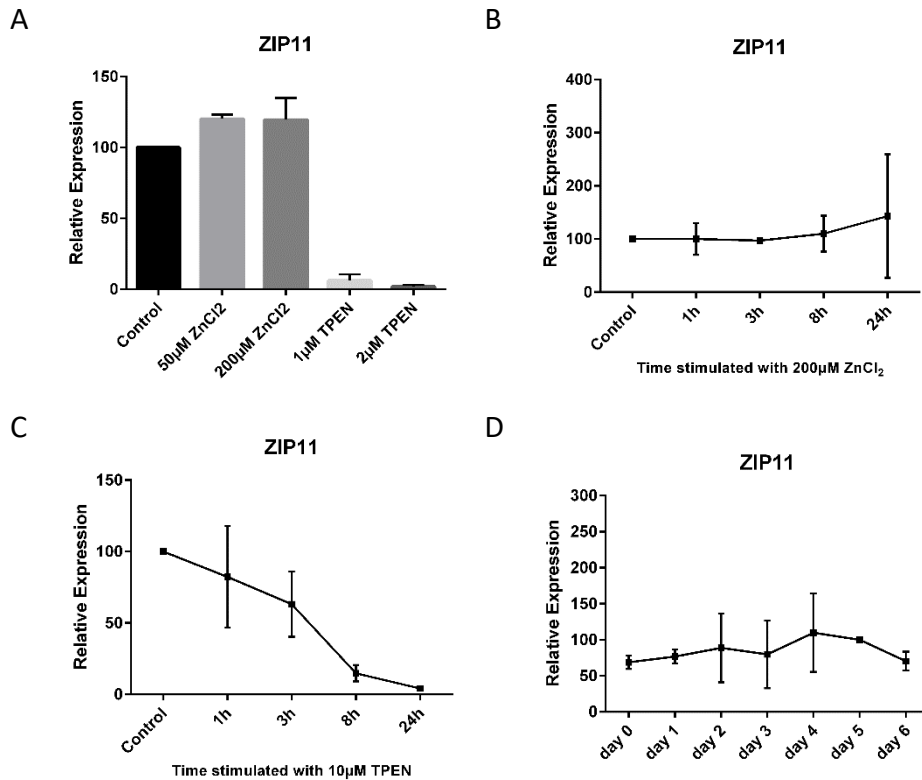


**Figure 15. Relative mRNA expression of *Slc39a11* (ZIP11) in mouse MKs.** (A) Relative mRNA expression of ZIP11 in mature primary MKs after 24h stimulation with different concentration of ZnCl<sub>2</sub> or TPEN. Control normalized to *Rplp0* was set to 100. (B) Relative mRNA expression of ZIP11 in mature MKs was followed at different time points (0, 1, 3, 8, 24 hours) in the presence of extracellular ZnCl<sub>2</sub> (200 μM) or (C) in the presence of TPEN (10 μM) Untreated control (0) normalized to *Rplp0* was set to 100. (D) Relative mRNA expression of ZIP11 was followed and stimulated with SCF (day 0 – 2), SCF/TPO (day 3 – 4) and TPO (day 5 - 6) during megakaryopoiesis. Day 5 values normalized to *Rplp0* were set to 100 (n ≥ 3, values: mean ± SEM).

### 3.3 Expression profile of *Slc30a* genes in mature megakaryocytes

The ZnT transporter family regulates  $Zn^{2+}$  efflux from the cytoplasm of cells. Quantitative (q) reverse transcriptase (RT)-PCR was performed using mRNAs isolated from primary mouse MKs at day 5. The amount of mRNA levels for all genes encoding ZnT transporters were compared to the housekeeping gene *Rplp0*, which was set to 100, according to the determined  $C_T$  values (Fig. 16)

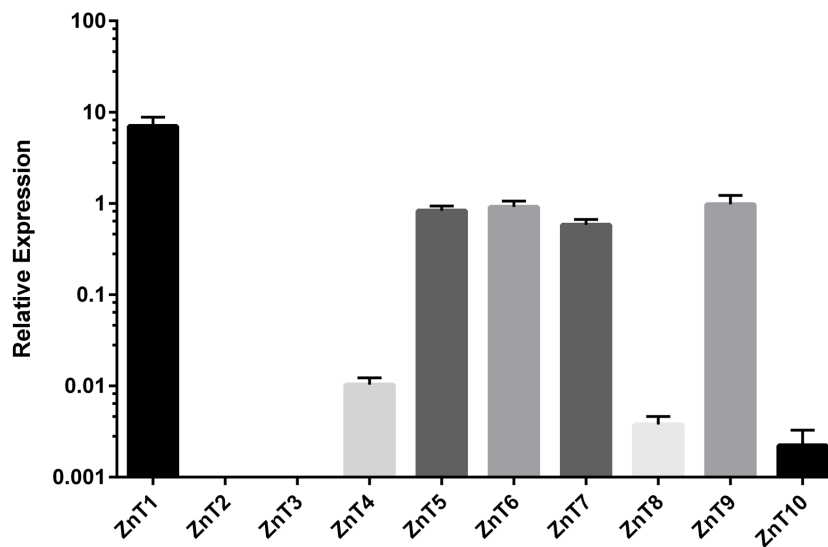


**Figure 16. Relative mRNA expression as determined by  $C_T$  values of *Slc30a* genes encoding ZnT transporters.** mRNA expression profile of mature MKs at day 5 relative to the mRNA level of *Rplp0*, whose expression was set to 100. Bar graphs are shown in logarithmic scale. ( $n \geq 3$  for every experiment, values: mean + SEM)

Similarly to ZIP transporters, ZnT transporters could be classified into three groups: (i) highly abundant expression (threshold: 1.5-fold lower than ZnT1), (ii) moderately (threshold: 15-fold lower than ZnT1), or (iii) the mRNA levels were low or extremely low (Table 2). ZnT1 (*Slc30a1*) was the highest expressed  $Zn^{2+}$  transporter (7 %) of all ten ZnT transporters and according to the  $C_T$  value 3.6-fold higher expressed than ZIP1.



Isoforms	Relative expression to ZnT1 (-fold)	Classification
ZnT2	Not detectable	iii
ZnT3	Not detectable	iii
ZnT4	↓ 684	iii
ZnT5	↓ 8.5	ii
ZnT6	↓ 7.7	ii
ZnT7	↓ 12	ii
ZnT8	↓ 1800	iii
ZnT9	↓ 7.2	ii
ZnT10	↓ 3000	iii

**Table 2. Relative expression of ZnT isoforms.** ZnT1 was compared to other ZnT isoforms.

Abundance of ZnT transporters ZnT5 (*Slc30a5*), ZnT6 (*Slc30a6*) and ZnT9 (*Slc30a9*) was quite similar (ZnT5: 8.5-fold lower than ZnT1, ZnT6: 7.7-fold lower than ZnT1, ZnT9: 7.2-fold lower than ZnT1) and classified “moderately expressed (ii)” when compared to ZnT1. ZnT7 (*Slc30a7*) expression in MKs was 12-fold lower than ZnT1 expression but was assigned to the “moderately expressed (ii)” group as well.

mRNA expression levels of the remaining ZnT isoforms ZnT4 (*Slc30a4*), ZnT8 (*Slc30a8*) and ZnT10 (*Slc30a10*) were in the range of approximately 680-fold to 3000-fold lower than ZnT1 expression (ZnT4: 684-fold lower, ZnT8: 1800-fold lower, ZnT10: 3000-fold lower) and therefore grouped to the “very low expressed (iii)” category. ZnT2 (*Slc30a2*) and ZnT3 (*Slc30a3*) were not detected in MKs.

### 3.3.1 Regulation of *Slc30a1* (ZnT1)

Transcriptional expression of *Slc30a1* as determined by mRNA levels was predominant compared to other ZnT transporters. *Slc30a1* showed a unique expression profile in MKs. Zn<sup>2+</sup> supplementation induced a dose-dependent increase in *Slc30a1* mRNA expression, indicating an important role of *Slc30a1* in Zn<sup>2+</sup> efflux, decreasing intracellular Zn<sup>2+</sup> content. Zn<sup>2+</sup> supplementation 50µM

ZnCl<sub>2</sub> resulted in 1.5-fold upregulation (p=0.18) of *Slc30a1* mRNA expression, treatment with 200µM ZnCl<sub>2</sub> increased mRNA expression even by 2.3-fold (p=0.07) (Fig. 17A)

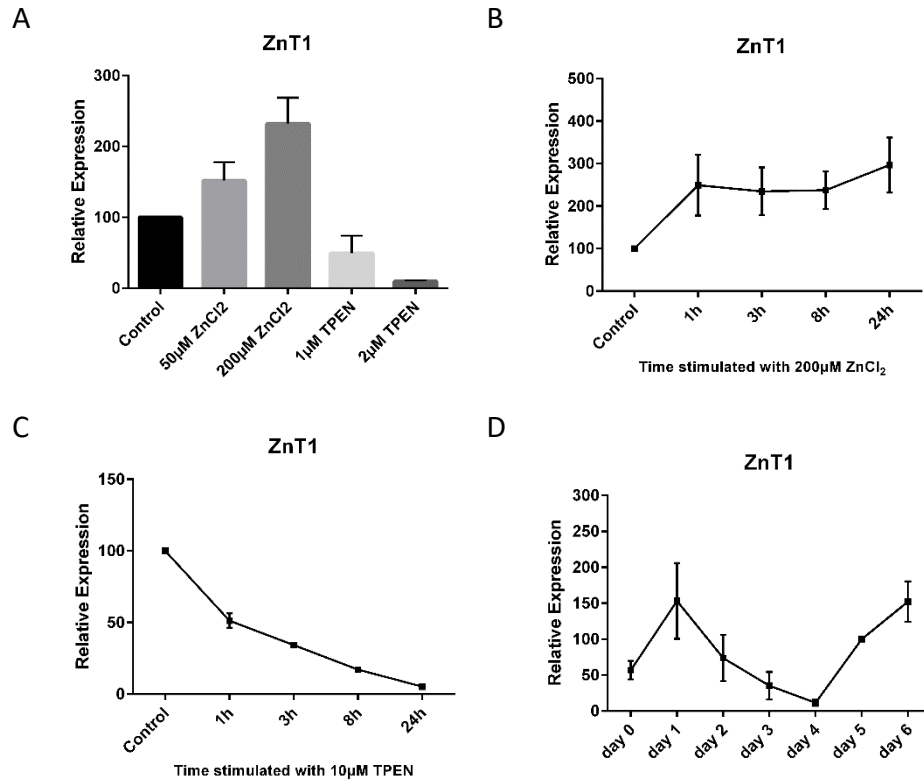


**Figure 17. Relative mRNA expression of *Slc30a1* (ZnT1) in mouse MKs.** (A) Relative mRNA expression of ZnT1 in mature primary MKs after 24h stimulation with different concentration of ZnCl<sub>2</sub> or TPEN. Control normalized to *Rplp0* was set to 100. (B) Relative mRNA expression of ZnT1 in mature MKs was followed at different time points (0, 1, 3, 8, 24 hours) in the presence of extracellular ZnCl<sub>2</sub> (200 µM) or (C) in the presence of TPEN (10 µM). Untreated control (0) normalized to *Rplp0* was set to 100. (D) Relative mRNA expression of ZnT1 was followed and stimulated with SCF (day 0 – 2), SCF/TPO (day 3 – 4) and TPO (day 5 - 6) during megakaryopoiesis. Day 5 values normalized to *Rplp0* were set to 100 (n≥ 3, values: mean ± SEM).

When followed up at ascending time points after Zn<sup>2+</sup> supplementation, 200µM ZnCl<sub>2</sub> lead to 2.5-fold upregulation after 1h and slightly increases to 3.0-fold (p=0.09) until 24h (Fig. 17B). Treatment of MKs with 1 µM TPEN did change mRNA expression slightly, but 2 µM TPEN strongly decreased mRNA expression by 10-fold (p<0.05) (Fig. 17A) and stimulation with 10µM TPEN induced a decrease in mRNA expression by 18.6-fold after 24h (p<0.05) (Fig. 17C). During megakaryopoiesis, mRNA expression level of *Slc30a1* was strongly regulated by

SCF and TPO. Relatively high expression was detected in the presence of SCF, but mRNA level was strongly downregulated in the presence of SCF and TPO by 13.2-fold ( $p=0.05$ ). When TPO alone was supplemented in the medium, mRNA level of *Slc30a1* was increased again by 13.1-fold ( $p<0.05$ ), indicating a time-dependent regulation of *Slc30a1* in megakaryopoiesis (Fig.17D).

### 3.3.2 Regulation of *Slc30a5* (ZnT5)

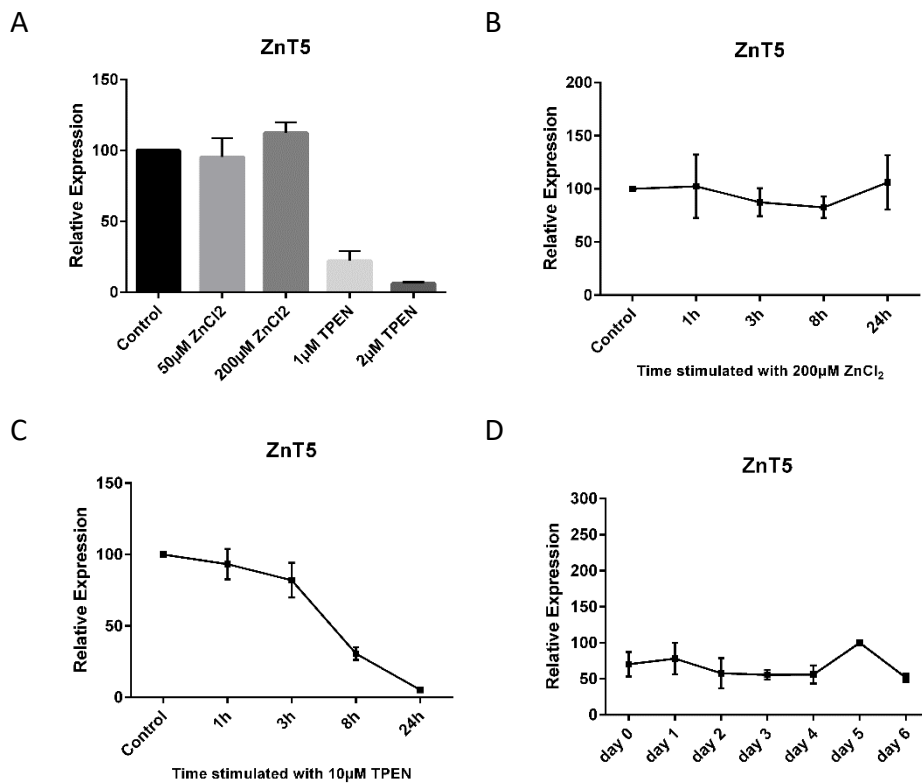


**Figure 18. Relative mRNA expression of *Slc30a5* (ZnT5) in mouse MKs.** (A) Relative mRNA expression of ZnT5 in mature primary MKs after 24h stimulation with different concentration of ZnCl<sub>2</sub> or TPEN. Control normalized to Rplp0 was set to 100. (B) Relative mRNA expression of ZnT5 in mature MKs was followed at different time points (0, 1, 3, 8, 24 hours) in the presence of extracellular ZnCl<sub>2</sub> (200 μM) or (C) in the presence of TPEN (10 μM). Untreated control (0) normalized to *Rplp0* was set to 100. (D) Relative mRNA expression of ZnT5 was followed and stimulated with SCF (day 0 – 2), SCF/TPO (day 3 – 4) and TPO (day 5 - 6) during megakaryopoiesis. Day 5 values normalized to *Rplp0* were set to 100 ( $n \geq 3$ , values: mean  $\pm$  SEM).

ZnT5 appears to be moderately expressed in MKs. Stimulation of mRNA expression with ZnCl<sub>2</sub> was insufficient to change expression of *Slc30a5* in MKs

(Fig. 18 A, B). However, dose-dependent inhibition was found after TPEN treatment (1  $\mu\text{M}$  TPEN: 4.5-fold ( $p < 0.05$ ), 2  $\mu\text{M}$  TPEN: 16-fold ( $p < 0.05$ )) (Fig. 18 A). MK treatment with 10  $\mu\text{M}$  TPEN lead to a strong downregulation of *Slc30a5* mRNA expression by 19-fold after 24h ( $p < 0.05$ ) (Fig. 18C). *Slc30a5* mRNA expression level did not change during megakaryopoiesis (Fig. 18D).

### 3.3.3 Regulation of *Slc30a6* (ZnT6)

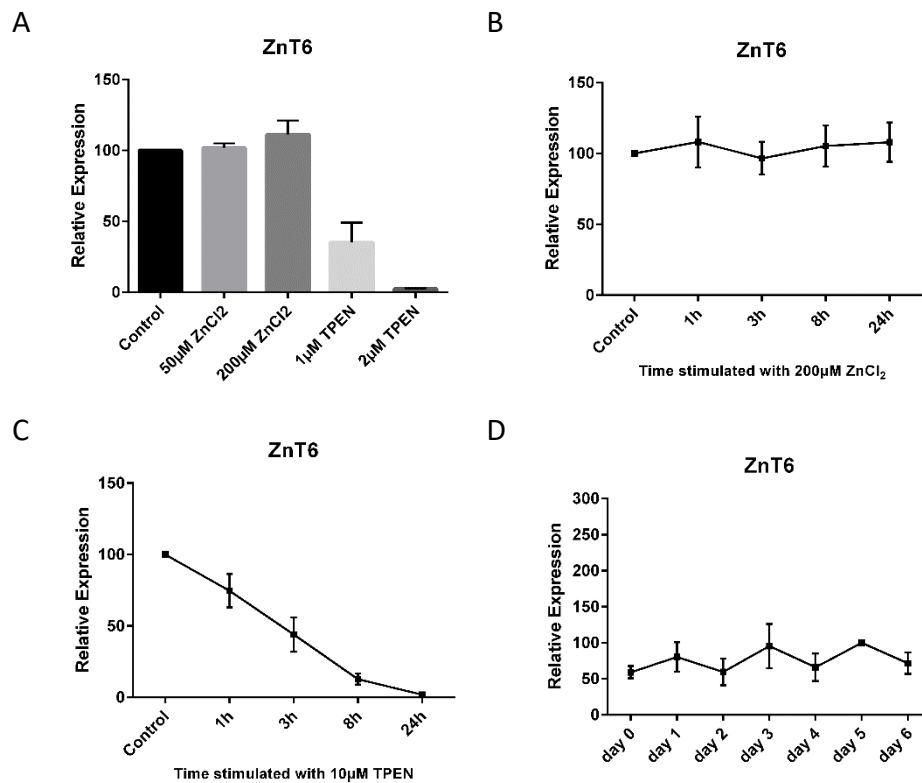


**Figure 19. Relative mRNA expression of *Slc30a6* (ZnT6) in mouse MKs.** (A) Relative mRNA expression of ZnT6 in mature primary MKs after 24h stimulation with different concentration of ZnCl<sub>2</sub> or TPEN. Control normalized to *Rplp0* was set to 100. (B) Relative mRNA expression of ZnT6 in mature MKs was followed at different time points (0, 1, 3, 8, 24 hours) in the presence of extracellular ZnCl<sub>2</sub> (200  $\mu\text{M}$ ) or (C) in the presence of TPEN (10  $\mu\text{M}$ ). Untreated control (0) normalized to *Rplp0* was set to 100. (D) Relative mRNA expression of ZnT6 was followed and stimulated with SCF (day 0 – 2), SCF/TPO (day 3 – 4) and TPO (day 5 - 6) during megakaryopoiesis. Day 5 values normalized to *Rplp0* were set to 100 ( $n \geq 3$ , values: mean  $\pm$  SEM).

*Slc30a6* appears to be moderately expressed in MKs. Zn<sup>2+</sup> supplementation with 50  $\mu\text{M}$  ZnCl<sub>2</sub> or 200  $\mu\text{M}$  ZnCl<sub>2</sub> did not alter mRNA expression of *Slc30a6* in MKs

(Fig. 19A, B). However, TPEN inhibited expression in a dose-dependent manner (1  $\mu\text{M}$  TPEN: 2.8-fold, 2  $\mu\text{M}$  TPEN:40-fold ( $p < 0.05$ )) (Fig. 19A).

Stimulation of MKs with 10  $\mu\text{M}$  TPEN resulted in a decrease of mRNA expression by 51.8-fold after 24h ( $p < 0.05$ ) (Fig. 19C). *Slc30a6* mRNA expression did not change during MK differentiation (Fig. 19D).

### 3.3.4 Regulation of *Slc30a7* (ZnT7)

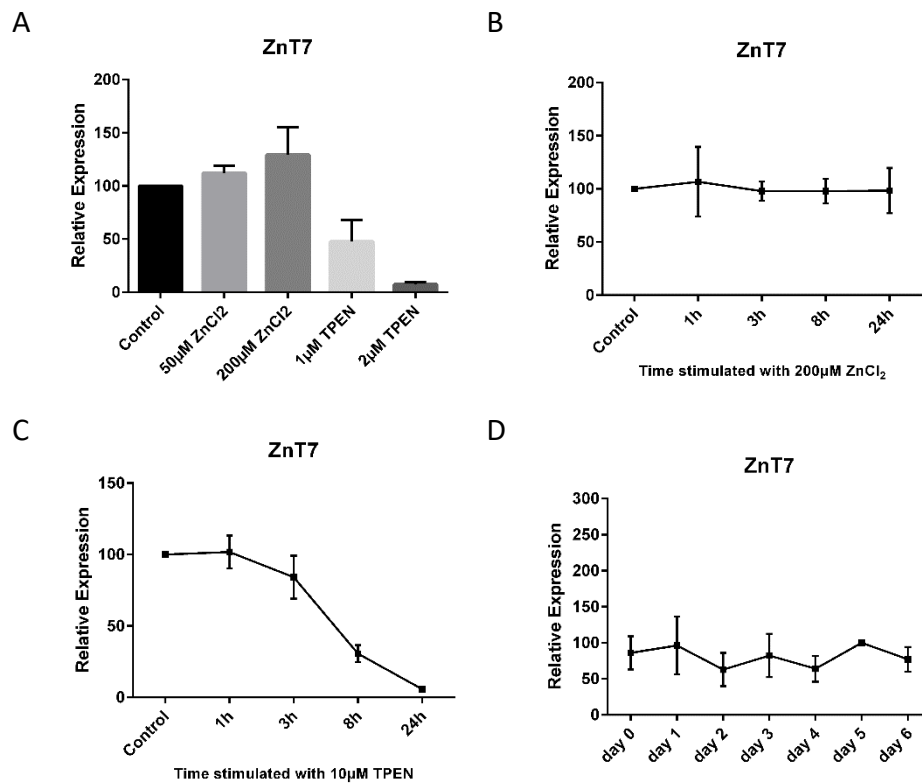


**Figure 20. Relative mRNA expression of *Slc30a7* (ZnT7) in mouse MKs.** (A) Relative mRNA expression of ZnT7 in mature primary MKs after 24h stimulation with different concentration of ZnCl<sub>2</sub> or TPEN. Control normalized to *Rplp0* was set to 100. (B) Relative mRNA expression of ZnT7 in mature MKs was followed at different time points (0, 1, 3, 8, 24 hours) in the presence of extracellular ZnCl<sub>2</sub> (200  $\mu\text{M}$ ) or (C) in the presence of TPEN (10  $\mu\text{M}$ ). Untreated control (0) normalized to *Rplp0* was set to 100. (D) Relative mRNA expression of ZnT7 was followed and stimulated with SCF (day 0 – 2), SCF/TPO (day 3 – 4) and TPO (day 5 - 6) during megakaryopoiesis. Day 5 values normalized to *Rplp0* were set to 100 ( $n \geq 3$ , values: mean  $\pm$  SEM).

*Slc30a7* is one of the moderately expressed genes from the *Slc30a* family in MKs. Zn<sup>2+</sup> supplementation did not change the mRNA levels of this gene while TPEN

treatment decreased expression of *Slc30a7* dose-dependent moderately or strongly (1  $\mu\text{M}$  TPEN: 2.1-fold,  $p=0.08$ ; 2  $\mu\text{M}$  TPEN: 13.5-fold,  $p<0.05$ ) (Fig. 20A, B). In mature MKs, 10  $\mu\text{M}$  TPEN resulted in a decrease of mRNA expression by 17.3-fold after 24h ( $p<0.05$ ) (Fig. 20C). During megakaryopoiesis, no significant changes in mRNA levels were observed (Fig. 20D).

### 3.3.5 Regulation of *Slc30a9* (ZnT9)

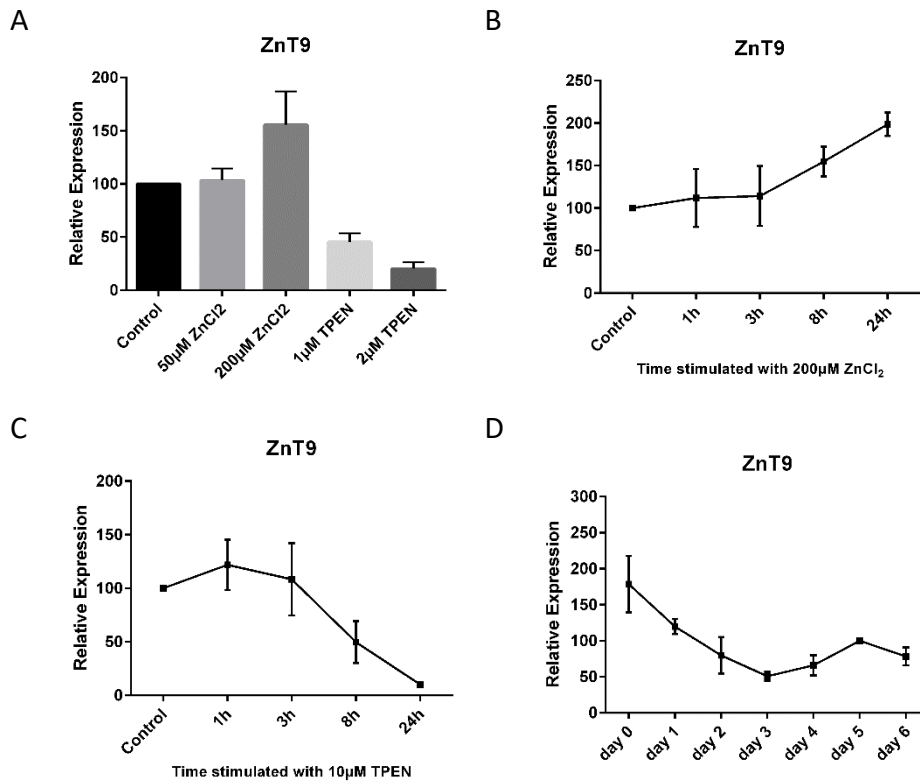


**Figure 21. Relative mRNA expression of *Slc30a9* (ZnT9) in mouse MKs.** (A) Relative mRNA expression of ZnT9 in mature primary MKs after 24h stimulation with different concentration of ZnCl<sub>2</sub> or TPEN. Control normalized to *Rplp0* was set to 100. (B) Relative mRNA expression of ZnT9 in mature MKs was followed at different time points (0, 1, 3, 8, 24 hours) in the presence of extracellular ZnCl<sub>2</sub> (200  $\mu\text{M}$ ) or (C) in the presence of TPEN (10  $\mu\text{M}$ ). Untreated control (0) normalized to *Rplp0* was set to 100. (D) Relative mRNA expression of ZnT9 was followed and stimulated with SCF (day 0 – 2), SCF/TPO (day 3 – 4) and TPO (day 5 - 6) during megakaryopoiesis. Day 5 values normalized to *Rplp0* were set to 100 ( $n \geq 3$ , values: mean  $\pm$  SEM).

*Slc30a9* appears to be moderately expressed in MKs. Treatment of MKs with 50  $\mu\text{M}$  ZnCl<sub>2</sub> did not change the mRNA level, while 200  $\mu\text{M}$  ZnCl<sub>2</sub> upregulates the

mRNA level by 1.5-fold. It is important to note that this result was variable and therefore not significant ( $p=0,22$ ) (Fig. 21A). In mature MKs, 200  $\mu\text{M}$   $\text{ZnCl}_2$  resulted in a 2.0-fold increase after 24h ( $p<0.05$ ) (Fig. 21B). TPEN treatment inhibited *Slc30a9* expression in a dose-dependent manner (1  $\mu\text{M}$  TPEN: 2.2-fold, 2  $\mu\text{M}$  TPEN: 5-fold ( $p<0.05$ )) (Fig. 21A). In mature MKs, 10  $\mu\text{M}$  TPEN treatment decreased *Slc30a9* mRNA expression by 9.8-fold after 24h ( $p<0.05$ ) (Fig. 21C). During megakaryopoiesis, mRNA expression level decreased by 3.5-fold until day 3 ( $p<0.05$ ) and slightly increased by 2.0-fold until day 5 of megakaryopoiesis ( $p<0.05$ ) (Fig. 21D).

## 4. Discussion

### 4.1 Extracellular Zn<sup>2+</sup> concentration strongly influences megakaryopoiesis

In the present work, hematopoietic stem cells isolated from murine bone marrow were differentiated to megakaryocytes (MKs) according to the protocol by Schulze *et al.* (104) After 6 days, differentiated cells showed the typical size and structure of MKs upon examination by transmission light microscopy and expressed the markers CD41 and CD42b, proteins that play crucial roles in hemostasis and are found in MKs and platelets abundantly (Fig. 4), indicating a successful differentiation process (97). Then the effects of Zn<sup>2+</sup> supplementation or deficiency MK development were investigated. In human blood plasma, the average concentration of Zn<sup>2+</sup> is about 15µM (9). Mammalian cells can tolerate higher doses of Zn<sup>2+</sup> up to 125 µM before they start to die. Earlier studies indicated that Zn<sup>2+</sup> deficiency induced by the Zn<sup>2+</sup> chelator TPEN at concentrations of 5-10 µM resulted in cell death (66).

In contrast to other mammalian cells, we observed that bone marrow derived MKs could tolerate Zn<sup>2+</sup> concentration up to 200 µM without showing any obvious signs of cell death. In addition, mRNA expression of *Gp1ba*, *Itga2b* and survival marker *Bcl2l1* even increased when compared to the control cells receiving medium without Zn<sup>2+</sup> supplements. This fits to the early results of Marx *et. al* (101) that platelets store Zn<sup>2+</sup> intracellularly, a finding recently confirmed by Gotru *et al.* (116) for MKs as well, indicating an important role of Zn<sup>2+</sup> in MK function and cell survival (Fig. 5). It is important to note that when cells were treated with 500µM ZnCl<sub>2</sub>, MKs became apoptotic (data not shown). Interestingly, when MKs were treated with Zn<sup>2+</sup> chelator TPEN, MKs started to die at lower concentrations (1-2 µM) compared to earlier studies using different cell types (66). However the cell culture media of these studies contained 6 µM Zn<sup>2+</sup>, which is in contrast to the Zn<sup>2+</sup> free medium of the present study, impeding the comparison of both results. The relative expression of the examined markers of *Bcl2l1*, *Gp1ba* and *Itga2b* decreased even at TPEN concentrations of 1-2 µM. MKs frequently form blebs and show abnormal plasma membrane structure, indicating a dramatic change of actin cytoskeleton and an instable membrane compartment (Fig. 6). Earlier, it



has been described that TPEN can induce transcriptional expression of Zn<sup>2+</sup> transporter genes (66), but here only downregulation of all tested Zn<sup>2+</sup> transporters was detected under these experimental conditions. It was concluded that using 1-2µM TPEN was not appropriate to simulate a moderate Zn<sup>2+</sup> deficit in MKs without inducing cell death under these experimental conditions. The cell culture medium used for the experiments of the present study did not contain Zn<sup>2+</sup>, therefore, lower concentrations of TPEN (0.1-0.5µM) or alternatively a combination of ZnCl<sub>2</sub> with TPEN should be tested in the near future, titrating an adequate concentration to avoid cellular toxicity.

#### **4.2 Transcriptional expression of genes encoding for ZIP proteins in MKs**

So far, the gene expression profile of zinc transporters in MKs has not been investigated. In most mammalian cell types, ZIP1 is a dominant transporter of the ZIP family (117), and in agreement with these findings, we also found the highest amounts of *Slc39a1* mRNA in MKs as well (Fig. 7). The increase of mRNA encoding for ZIP1 after addition of TPO at day 5 and 6 indicates an important regulatory role of ZIP1 in Zn<sup>2+</sup> uptake of MKs. Zn<sup>2+</sup> supplementation did not change mRNA expression of this gene (Fig. 8). This observation is in line with other published results that *Slc39a1* mRNA level is not regulated by Zn<sup>2+</sup>. Dufner-Beattie *et al.* showed this for dietary Zn<sup>2+</sup> deficiency in murine small intestine and visceral yolk sac (17), Cousins *et al.* for human THP-1 monocytes (118) and Wang *et al.* showed in HEK293 cells that a mechanism of Zn<sup>2+</sup> stimulated endocytosis controls ZIP1 activity instead (18). Nevertheless, ZIP1 is potentially an interesting subject for further studies in MKs, regarding subcellular localization and involvement of Zn<sup>2+</sup> uptake at late steps of megakaryopoiesis.

ZIP2 (*Slc39a2*) expression is very restricted to few organs (21), and *Slc39a2* mRNA was not expressed in mouse MKs, indicating a dispensable role of this transporter in MK Zn<sup>2+</sup> homeostasis. Therefore, ZIP2 was not further investigated in the present study.

Similar to ZIP2, the *Slc39a3* (ZIP3) gene has also a restricted tissue specific expression. However, this transporter was moderately expressed in MKs (Fig. 7). Zn<sup>2+</sup> status of the cell does not alter expression of *Slc39a3* mRNA (Fig. 9) and

this finding was in agreement with other results observed in different cell types. Again, Dufner-Beattie *et al.* (17) and Cousins *et al.* (118) showed this for mouse small intestine and visceral yolk sac or for human THP-1 monocytes, respectively, and Wang *et al.* demonstrated in HEK293 a mechanism of Zn<sup>2+</sup> stimulated endocytosis for control of ZIP3 activity (18). In addition, a slight upregulation of *Slc39a3* mRNA expression was found at the end of megakaryopoiesis (Fig. 9), which indicates that this gene may play some role at late stages of MK development. Therefore, its specific role in MKs has to be further investigated.

Also, a moderate gene expression of *Slc39a4* (ZIP4) was observed in MKs (Fig. 7). Again, only little alteration of gene expression was induced by Zn<sup>2+</sup> supplementation (Fig. 10), which was also observed in THP-1 cells in an earlier publication (118). However, these findings are in contrast to Dufner-Beattie *et al.* who showed strong upregulation of *Slc39a4* mRNA levels induced by dietary Zn<sup>2+</sup> deficiency in mouse small intestine (25). This indicates cell type specific differences in regulation of this gene. Interestingly, a strong upregulation of *Slc39a4* was detected during late stages of megakaryopoiesis (Fig. 10), indicating an important role of ZIP4 in MK maturation and possibly proplatelet formation, making this gene an interesting subject for further studies.

*Slc39a5* (ZIP5) appears to be also expressed in MKs, although on a very low level (Fig. 7), which is in line with studies that show a specific expression of this gene in tissues such as pancreas (30). Therefore, it is concluded that ZIP5 seems not to be a crucial regulator of Zn<sup>2+</sup> uptake in MKs.

*Slc39a6* (ZIP6) was found to be moderately expressed in MKs on mRNA level (Fig. 7). However, expression remained nearly on the same level during megakaryopoiesis. Under zinc excess conditions, a slight downregulation of gene transcription could be observed (Fig. 11). The exact role of ZIP6 in MK zinc homeostasis has to be investigated in further studies.

*Slc39a7* (ZIP7) is widely expressed in mammalian tissues, and high expression levels of its mRNA were also detected in MKs (Fig. 7). However, the gene expression is not altered in the presence of Zn<sup>2+</sup> supplement or during megakaryopoiesis (Fig. 12). This was also observed earlier in the human prostate

cell line RWPE1 cells by Huang *et al.*, who showed that ZIP7 protein expression is translationally regulated by Zn<sup>2+</sup> instead (36). The exact role of ZIP7 in MKs will have to be enlightened in further studies.

*Slc39a8* (ZIP8) is expressed on a very low level in MKs according to the presence of *Slc39a8* mRNA (Fig. 7), indicating a dispensable role in this cell type. Therefore, the gene expression was not examined further in this study.

The *Slc39a9* gene (ZIP9) is similarly to *Slc39a1* and *Slc39a7* a highly expressed Zn<sup>2+</sup> transporter in MKs (Fig. 7). However, gene expression was not altered significantly during megakaryopoiesis and no significant change in mRNA expression was found in the presence of Zn<sup>2+</sup> supplement (Fig. 13). This finding was in line with the publication of Matsuura *et al.*, who showed that the ZIP9 protein level and its subcellular localization were not influenced by cellular Zn<sup>2+</sup> status in HeLa cells (57).

*Slc39a10* (ZIP10) was found to be moderately expressed in MKs (Fig. 7), and interestingly, *Slc39a10* mRNA levels were downregulated in the presence of Zn<sup>2+</sup> supplementation (Fig. 14). Zn<sup>2+</sup> dependent gene regulation was also observed in other cell types in earlier studies: Lichten *et al.* showed that *Slc39a10* mRNA levels of AML12 hepatocytes declined when Zn<sup>2+</sup> was supplemented (45). Given the fact that ZIP10 is located in the plasma membrane, this finding suggests that ZIP10 might be a key regulator of Zn<sup>2+</sup> uptake in MKs, and the suppression of its transcription in the presence of excessive Zn<sup>2+</sup> may be important to protect MKs from extracellular Zn<sup>2+</sup> toxicity. Therefore, further investigations on the relevance of this transporter in MKs using MK/platelet-specific knockout mouse lines would be an interesting subject in the near future.

The *Slc39a11* gene (ZIP11) was found to be moderately expressed in MKs (Fig. 7), and no alterations of mRNA expression were found in the presence of Zn<sup>2+</sup> supplementation and during megakaryopoiesis (Fig. 15). The exact role of ZIP11 in MK Zn<sup>2+</sup> homeostasis has to be investigated in further studies.

Transcription of *Slc39a12* (ZIP12), *Slc39a13* (ZIP13), and *Slc39a14* (ZIP14) was found to be very low in MKs according to hardly detectable mRNA levels (Fig. 7), indicating a dispensable role of these transporters in MKs.

### 4.3 Transcriptional expression of genes encoding for ZnT proteins in MKs

We found that the highest expressed *Slc30a* (ZnT) transporter gene in MKs is *Slc30a1* (ZnT1) (Fig. 16). Under  $Zn^{2+}$  supplementation the expression of *Slc30a1* mRNA increased in MKs (Fig. 17), which was also observed in other cell types in earlier studies. Tsuda *et al.* showed this effect in rat hippocampal neurons (119) and Langmade *et al.* for murine hepatoma cells (Hepa) and mouse embryo fibroblasts (61). ZnT1 regulation is likely one of the most important mechanisms for keeping the equilibrium of  $Zn^{2+}$  homeostasis in MKs by increasing  $Zn^{2+}$  efflux. The genes of *Slc30a2* (ZnT2), *Slc30a3* (ZnT3) and *Slc30a4* (ZnT4) were found to be expressed at very low levels in MKs (Fig. 16), Therefore it is concluded that these genes do not play important roles in  $Zn^{2+}$  homeostasis of MKs.

*Slc30a5* (ZnT5) was found to be moderately expressed in MKs (Fig. 16). However, no alteration of mRNA levels was found under  $Zn^{2+}$  supplementation (Fig. 18), which was in agreement with a previous study that showed the same result in HeLa cells (66).

ZnT6 lacks  $Zn^{2+}$  transport ability, however, it forms heterodimers with ZnT5 and it has been proposed that it is modulating  $Zn^{2+}$  transport of ZnT5 (79). *Slc30a6* (ZnT6) was also found to be expressed on the same moderate level as *Slc30a5* in MKs (Fig. 16). However,  $Zn^{2+}$  supplementation did not affect gene expression of this transporter in MKs (Fig. 19), a result that has also been shown by Cousins *et al.* in THP-1 monocytes in an earlier study (118). ZnT6 function appears to be regulated differently, subcellular localization of the protein might change  $Zn^{2+}$  homeostasis in the cell (81).

The *Slc30a7* (ZnT7) gene is expressed moderately in murine primary MKs (Fig. 16). However, mRNA level of *Slc30a7* is stable during megakaryopoiesis and during  $Zn^{2+}$  supplementation (Fig. 20). It has been reported that, similarly to *Slc30a6*, subcellular re-localization of the protein can induce change in  $Zn^{2+}$  homeostasis (66, 83).

*Slc30a8* (ZnT8) was detected mainly in pancreatic  $\beta$ -cells (87). Consequently, *Slc30a8* mRNA expression was found to be very low in MKs, indicating that this gene does not play a role in MK  $Zn^{2+}$  homeostasis.

*Slc30a9* (ZnT9) gene was found to be expressed moderately in MKs (Fig. 16). Furthermore, gene expression of *Slc30a9* appears to be strongly regulated during megakaryopoiesis (Fig. 21). However, it is lacking the intracellular binding site for  $Zn^{2+}$  and its plasma membrane localization was ruled out (2). Therefore it is unlikely that this protein regulates  $Zn^{2+}$  transport at the plasma membrane. It has been shown that ZnT9 plays a role in nuclear receptor coactivation (89).

The gene of *Slc30a10* (ZnT10) is expressed at a very low level in MKs, indicating a negligible function of this transporter in the regulation of  $Zn^{2+}$  transport mechanism in MKs.

#### **4.5 Outlook**

The present work has given a first overview of *Slc39a/Slc30a* (ZIP/ZnT) gene expression in MKs. Using systematic analyses with quantitative RT-PCR some interesting candidate genes for ZIP/ZnT proteins were detected, which were regulated by extracellular  $Zn^{2+}$  or during megakaryopoiesis under *in vitro* conditions. However, this is only the first step to understand better how  $Zn^{2+}$  homeostasis is regulated in MKs. Follow-up studies are necessary to investigate  $Zn^{2+}$  dependent MK maturation and proplatelet formation, which may influence platelet production in mice.

In addition, regulatory mechanisms other than alteration of gene expression for both zinc excess and deficiency have to be examined. Biochemical analyses with Western blotting and immunostaining of intact cells will add important information how  $Zn^{2+}$  could regulate protein levels and subcellular localization of these proteins. Especially, it would be important to detect ZIP/ZnT proteins on the membrane of granules, since MKs and platelets can take up and store  $Zn^{2+}$  in these organelles. Ultimately, genetic mouse models with MK/platelet-specific loss of individual zinc transporters will clarify their importance for MK and platelet function *in vivo*. This information might help to identify abnormal  $Zn^{2+}$  transport mechanisms in disease conditions, especially in patients with storage pool disorders with abnormal granule development.

## 5. Summary

Zinc is an essential trace element for all living organisms. In mammals, including humans and mice, it is required for normal growth, development, hematopoiesis and immune defense. This thesis investigates the influence of zinc on the development of megakaryocytes (MKs), the cells responsible for bone marrow-derived platelet production. Furthermore, a detailed analysis of the expression of zinc import and export transporters (*Slc39a/Slc30a* genes) is carried out, firstly over the course of MK differentiation and secondly dependent on extracellular zinc.

In order to study MKs *in vitro*, they were differentiated from murine bone marrow stem cells by stimulation with thrombopoietin. First of all, it could be shown that the murine MKs are able to tolerate high extracellular zinc concentrations without being restricted in their development, suggesting that these cells have a very effective zinc redistribution or export system. Conversely, even the smallest amounts of the zinc-specific chelator N,N,N',N'-tetrakis(2-pyridylmethyl)-ethylene-diamine (TPEN) had a toxic effect and led to the death of the examined cells, which in turn emphasizes that zinc is essential for the development of MKs. Five out of ten members of the *Slc30a* gene family (encoding ZnT proteins) responsible for the export of zinc from the cytosol into the extracellular space or into organelles were expressed to a relevant amount in murine MKs, of which in turn the genes *Slc30a1* and *Slc30a9* were regulated at the mRNA level over the course of MK differentiation and in presence of extracellular zinc.

Eight out of fourteen members of the *Slc39a* gene family (encoding ZIP proteins) responsible for the import of zinc into the cytosol reach relevant mRNA levels in MKs. For the genes *Slc39a1*, *Slc39a3*, *Slc39a4*, *Slc39a6* and *Slc39a10* regulation at mRNA level could be shown either over the course of MK differentiation or in presence of extracellular zinc.

This work contributes to the understanding of the distribution mechanisms of zinc in MKs and thus ultimately to the elucidation of the role of zinc in hemostasis.

## 5. Zusammenfassung

Zink ist ein für alle lebenden Organismen essentiell wichtiges Spurenelement. Bei Säugetieren, einschließlich Menschen und Mäusen, ist es für normales Wachstum, die normale Entwicklung, Hämatopoese und Immunantwort erforderlich. Diese Arbeit untersucht den Einfluss von Zink auf die Entwicklung von Megakaryozyten (MKs), derjenigen Zellen, welche für die Produktion der Thrombozyten im Knochenmark verantwortlich sind. Darüber hinaus wird eine detaillierte Analyse der Expression von Zinkimporttransportern und Zinkexporttransportern (*Slc39a* / *Slc30a*-Gene) durchgeführt, zum einen im Verlauf der MK-Differenzierung und zum anderen in Abhängigkeit von extrazellulärem Zink.

Um MKs *in vitro* zu untersuchen, wurden sie durch Stimulation mit Thrombopoetin aus murinen Knochenmarksstammzellen differenziert. Zunächst konnte gezeigt werden, dass die murinen MKs in der Lage sind, auch unphysiologisch hohe extrazelluläre Zinkkonzentrationen zu tolerieren, ohne in ihrer Entwicklung eingeschränkt zu sein, was darauf hinweist, dass diese Zellen über ein sehr effektives Umverteilungs- beziehungsweise Exportsystem für Zink verfügen. Umgekehrt wirkten selbst kleinste Mengen des Zink-spezifischen Chelators N,N,N',N'-Tetrakis(2-pyridylmethyl)-ethylen-diamin (TPEN) toxisch und führten zum Tod der untersuchten Zellen, was wiederum hervorhebt, dass Zink essentiell für die Entwicklung der MKs ist.

Fünf von zehn Mitgliedern der *Slc30a*-Genfamilie (kodierend für ZnT-Proteine), die für den Export von Zink aus dem Zytosol in den Extrazellulärraum oder in Organellen verantwortlichen sind, wurden in murinen MKs in einer relevanten Menge exprimiert, wovon wiederum die Gene *Slc30a1* und *Slc30a9* auf mRNA-Ebene über den Verlauf der MK-Differenzierung und in Gegenwart von extrazellulärem Zink reguliert wurden.

Acht von vierzehn Vertretern der *Slc39a*-Genfamilie (kodierend für ZnT-Proteine), die für den Import von Zink in das Zytosol verantwortlichen sind, erreichen relevante mRNA-Spiegel in MKs. Für die Gene *Slc39a1*, *Slc39a3*, *Slc39a4*, *Slc39a6* und *Slc39a10* konnte eine Regulation auf mRNA-Ebene

entweder im Verlauf der MK-Differenzierung oder in Gegenwart von extrazellulärem Zink gezeigt werden.

Diese Arbeit trägt zum Verständnis der Verteilungsmechanismen von Zink in Megakaryozyten und damit letztlich zur Aufklärung der Rolle von Zink in der Hämostase bei.



## 6. References

1. Vallee BL, Falchuk KH. The biochemical basis of zinc physiology. *Physiol Rev* 1993;73:79-118.
2. Kambe T, Tsuji T, Hashimoto A, Itsumura N. The Physiological, Biochemical, and Molecular Roles of Zinc Transporters in Zinc Homeostasis and Metabolism. *Physiol Rev* 2015;95:749-784.
3. Tamaki M, Fujitani Y, Hara A, Uchida T, Tamura Y, Takeno K, Kawaguchi M, et al. The diabetes-susceptible gene SLC30A8/ZnT8 regulates hepatic insulin clearance. *J Clin Invest* 2013;123:4513-4524.
4. Wastney ME, Aamodt RL, Rumble WF, Henkin RI. Kinetic analysis of zinc metabolism and its regulation in normal humans. *Am J Physiol* 1986;251:R398-408.
5. Lee HH, Prasad AS, Brewer GJ, Owyang C. Zinc absorption in human small intestine. *Am J Physiol* 1989;256:G87-91.
6. Nishito Y, Kambe T. Absorption Mechanisms of Iron, Copper, and Zinc: An Overview. *J Nutr Sci Vitaminol (Tokyo)* 2018;64:1-7.
7. Hambidge M, Krebs NF. Interrelationships of key variables of human zinc homeostasis: relevance to dietary zinc requirements. *Annu Rev Nutr* 2001;21:429-452.
8. Reyes JG. Zinc transport in mammalian cells. *Am J Physiol* 1996;270:C401-410.
9. Foote JW, Delves HT. Albumin bound and alpha 2-macroglobulin bound zinc concentrations in the sera of healthy adults. *J Clin Pathol* 1984;37:1050-1054.
10. Plum LM, Rink L, Haase H. The Essential Toxin: Impact of Zinc on Human Health. *International Journal of Environmental Research and Public Health* 2010;7:1342-1365.
11. Chimienti F, Seve M, Richard S, Mathieu J, Favier A. Role of cellular zinc in programmed cell death: temporal relationship between zinc depletion, activation of caspases, and cleavage of Sp family transcription factors. *Biochem Pharmacol* 2001;62:51-62.
12. Fukamachi Y, Karasaki Y, Sugiura T, Itoh H, Abe T, Yamamura K, Higashi K. Zinc suppresses apoptosis of U937 cells induced by hydrogen peroxide through an increase of the Bcl-2/Bax ratio. *Biochem Biophys Res Commun* 1998;246:364-369.

13. Stuart GW, Searle PF, Palmiter RD. Identification of multiple metal regulatory elements in mouse metallothionein-I promoter by assaying synthetic sequences. *Nature* 1985;317:828-831.
14. Fischer EH, Davie EW. Recent excitement regarding metallothionein. *Proc Natl Acad Sci U S A* 1998;95:3333-3334.
15. Schlessinger A, Matsson P, Shima JE, Pieper U, Yee SW, Kelly L, Apeltsin L, et al. Comparison of human solute carriers. *Protein Sci* 2010;19:412-428.
16. Gueriot ML. The ZIP family of metal transporters. *Biochim Biophys Acta* 2000;1465:190-198.
17. Dufner-Beattie J, Langmade SJ, Wang F, Eide D, Andrews GK. Structure, function, and regulation of a subfamily of mouse zinc transporter genes. *J Biol Chem* 2003;278:50142-50150.
18. Wang F, Dufner-Beattie J, Kim BE, Petris MJ, Andrews G, Eide DJ. Zinc-stimulated endocytosis controls activity of the mouse ZIP1 and ZIP3 zinc uptake transporters. *J Biol Chem* 2004;279:24631-24639.
19. Gaither LA, Eide DJ. The human ZIP1 transporter mediates zinc uptake in human K562 erythroleukemia cells. *J Biol Chem* 2001;276:22258-22264.
20. Dufner-Beattie J, Huang ZL, Geiser J, Xu W, Andrews GK. Mouse ZIP1 and ZIP3 genes together are essential for adaptation to dietary zinc deficiency during pregnancy. *Genesis* 2006;44:239-251.
21. Peters JL, Dufner-Beattie J, Xu W, Geiser J, Lahner B, Salt DE, Andrews GK. Targeting of the mouse *Slc39a2* (*Zip2*) gene reveals highly cell-specific patterns of expression, and unique functions in zinc, iron, and calcium homeostasis. *Genesis* 2007;45:339-352.
22. Inoue Y, Hasegawa S, Ban S, Yamada T, Date Y, Mizutani H, Nakata S, et al. ZIP2 protein, a zinc transporter, is associated with keratinocyte differentiation. *J Biol Chem* 2014;289:21451-21462.
23. Dufner-Beattie J, Huang ZL, Geiser J, Xu W, Andrews GK. Generation and characterization of mice lacking the zinc uptake transporter ZIP3. *Mol Cell Biol* 2005;25:5607-5615.
24. Kambe T, Geiser J, Lahner B, Salt DE, Andrews GK. *Slc39a1* to 3 (subfamily II) *Zip* genes in mice have unique cell-specific functions during adaptation to zinc deficiency. *Am J Physiol Regul Integr Comp Physiol* 2008;294:R1474-1481.
25. Dufner-Beattie J, Wang F, Kuo YM, Gitschier J, Eide D, Andrews GK. The acrodermatitis enteropathica gene ZIP4 encodes a tissue-specific, zinc-regulated zinc transporter in mice. *J Biol Chem* 2003;278:33474-33481.

26. Dufner-Beattie J, Kuo YM, Gitschier J, Andrews GK. The adaptive response to dietary zinc in mice involves the differential cellular localization and zinc regulation of the zinc transporters ZIP4 and ZIP5. *J Biol Chem* 2004;279:49082-49090.
27. Wang F, Kim BE, Dufner-Beattie J, Petris MJ, Andrews G, Eide DJ. Acrodermatitis enteropathica mutations affect transport activity, localization and zinc-responsive trafficking of the mouse ZIP4 zinc transporter. *Hum Mol Genet* 2004;13:563-571.
28. Mao X, Kim BE, Wang F, Eide DJ, Petris MJ. A histidine-rich cluster mediates the ubiquitination and degradation of the human zinc transporter, hZIP4, and protects against zinc cytotoxicity. *J Biol Chem* 2007;282:6992-7000.
29. Geiser J, Venken KJ, De Lisle RC, Andrews GK. A mouse model of acrodermatitis enteropathica: loss of intestine zinc transporter ZIP4 (Slc39a4) disrupts the stem cell niche and intestine integrity. *PLoS Genet* 2012;8:e1002766.
30. Wang F, Kim BE, Petris MJ, Eide DJ. The mammalian Zip5 protein is a zinc transporter that localizes to the basolateral surface of polarized cells. *J Biol Chem* 2004;279:51433-51441.
31. Weaver BP, Dufner-Beattie J, Kambe T, Andrews GK. Novel zinc-responsive post-transcriptional mechanisms reciprocally regulate expression of the mouse Slc39a4 and Slc39a5 zinc transporters (Zip4 and Zip5). *Biol Chem* 2007;388:1301-1312.
32. Geiser J, De Lisle RC, Andrews GK. The zinc transporter Zip5 (Slc39a5) regulates intestinal zinc excretion and protects the pancreas against zinc toxicity. *PLoS One* 2013;8:e82149.
33. Hogstrand C, Kille P, Ackland ML, Hiscox S, Taylor KM. A mechanism for epithelial-mesenchymal transition and anoikis resistance in breast cancer triggered by zinc channel ZIP6 and STAT3 (signal transducer and activator of transcription 3). *Biochem J* 2013;455:229-237.
34. Taylor KM, Morgan HE, Johnson A, Hadley LJ, Nicholson RI. Structure-function analysis of LIV-1, the breast cancer-associated protein that belongs to a new subfamily of zinc transporters. *Biochem J* 2003;375:51-59.
35. Colomar-Carando N, Meseguer A, Company-Garrido I, Jutz S, Herrera-Fernandez V, Olvera A, Kiefer K, et al. Zip6 Transporter Is an Essential Component of the Lymphocyte Activation Machinery. *J Immunol* 2019;202:441-450.
36. Huang L, Kirschke CP, Zhang Y, Yu YY. The ZIP7 Gene (Slc39a7) Encodes a Zinc Transporter Involved in Zinc Homeostasis of the Golgi Apparatus. *Journal of Biological Chemistry* 2005;280:15456-15463.

37. Taylor KM, Hiscox S, Nicholson RI, Hogstrand C, Kille P. Protein kinase CK2 triggers cytosolic zinc signaling pathways by phosphorylation of zinc channel ZIP7. *Sci Signal* 2012;5:ra11.
38. Taylor KM, Morgan HE, Johnson A, Nicholson RI. Structure-function analysis of HKE4, a member of the new LIV-1 subfamily of zinc transporters. *Biochem J* 2004;377:131-139.
39. Ohashi W, Kimura S, Iwanaga T, Furusawa Y, Irie T, Izumi H, Watanabe T, et al. Zinc Transporter SLC39A7/ZIP7 Promotes Intestinal Epithelial Self-Renewal by Resolving ER Stress. *PLoS Genet* 2016;12:e1006349.
40. He L, Girijashanker K, Dalton TP, Reed J, Li H, Soleimani M, Nebert DW. ZIP8, member of the solute-carrier-39 (SLC39) metal-transporter family: characterization of transporter properties. *Mol Pharmacol* 2006;70:171-180.
41. Aydemir TB, Liuzzi JP, McClellan S, Cousins RJ. Zinc transporter ZIP8 (SLC39A8) and zinc influence IFN-gamma expression in activated human T cells. *J Leukoc Biol* 2009;86:337-348.
42. Jenkitkasemwong S, Wang CY, Mackenzie B, Knutson MD. Physiologic implications of metal-ion transport by ZIP14 and ZIP8. *Biometals* 2012;25:643-655.
43. Galvez-Peralta M, He L, Jorge-Nebert LF, Wang B, Miller ML, Eppert BL, Afton S, et al. ZIP8 zinc transporter: indispensable role for both multiple-organ organogenesis and hematopoiesis in utero. *PLoS One* 2012;7:e36055.
44. Koike A, Sou J, Ohishi A, Nishida K, Nagasawa K. Inhibitory effect of divalent metal cations on zinc uptake via mouse Zrt-/Irt-like protein 8 (ZIP8). *Life Sci* 2017;173:80-85.
45. Lichten LA, Ryu MS, Guo L, Embury J, Cousins RJ. MTF-1-mediated repression of the zinc transporter Zip10 is alleviated by zinc restriction. *PLoS One* 2011;6:e21526.
46. Miyai T, Hojyo S, Ikawa T, Kawamura M, Irie T, Ogura H, Hijikata A, et al. Zinc transporter SLC39A10/ZIP10 facilitates antiapoptotic signaling during early B-cell development. *Proc Natl Acad Sci U S A* 2014;111:11780-11785.
47. Kagara N, Tanaka N, Noguchi S, Hirano T. Zinc and its transporter ZIP10 are involved in invasive behavior of breast cancer cells. *Cancer Sci* 2007;98:692-697.
48. Bin BH, Bhin J, Takaishi M, Toyoshima KE, Kawamata S, Ito K, Hara T, et al. Requirement of zinc transporter ZIP10 for epidermal development: Implication of the ZIP10-p63 axis in epithelial homeostasis. *Proc Natl Acad Sci U S A* 2017;114:12243-12248.

49. Chowanadisai W, Graham DM, Keen CL, Rucker RB, Messerli MA. Neurulation and neurite extension require the zinc transporter ZIP12 (slc39a12). *Proc Natl Acad Sci U S A* 2013;110:9903-9908.
50. Fukada T, Civic N, Furuichi T, Shimoda S, Mishima K, Higashiyama H, Idaira Y, et al. The zinc transporter SLC39A13/ZIP13 is required for connective tissue development; its involvement in BMP/TGF-beta signaling pathways. *PLoS One* 2008;3:e3642.
51. Bin BH, Fukada T, Hosaka T, Yamasaki S, Ohashi W, Hojyo S, Miyai T, et al. Biochemical characterization of human ZIP13 protein: a homo-dimerized zinc transporter involved in the spondylocheiro dysplastic Ehlers-Danlos syndrome. *J Biol Chem* 2011;286:40255-40265.
52. Taylor KM, Morgan HE, Johnson A, Nicholson RI. Structure-function analysis of a novel member of the LIV-1 subfamily of zinc transporters, ZIP14. *FEBS Lett* 2005;579:427-432.
53. Liuzzi JP, Lichten LA, Rivera S, Blanchard RK, Aydemir TB, Knutson MD, Ganz T, et al. Interleukin-6 regulates the zinc transporter Zip14 in liver and contributes to the hypozincemia of the acute-phase response. *Proc Natl Acad Sci U S A* 2005;102:6843-6848.
54. Pinilla-Tenas JJ, Sparkman BK, Shawki A, Illing AC, Mitchell CJ, Zhao N, Liuzzi JP, et al. Zip14 is a complex broad-scope metal-ion transporter whose functional properties support roles in the cellular uptake of zinc and nontransferrin-bound iron. *Am J Physiol Cell Physiol* 2011;301:C862-871.
55. Zhao N, Zhang AS, Worthen C, Knutson MD, Enns CA. An iron-regulated and glycosylation-dependent proteasomal degradation pathway for the plasma membrane metal transporter ZIP14. *Proc Natl Acad Sci U S A* 2014;111:9175-9180.
56. Aydemir TB, Sitren HS, Cousins RJ. The zinc transporter Zip14 influences c-Met phosphorylation and hepatocyte proliferation during liver regeneration in mice. *Gastroenterology* 2012;142:1536-1546 e1535.
57. Matsuura W, Yamazaki T, Yamaguchi-Iwai Y, Masuda S, Nagao M, Andrews GK, Kambe T. SLC39A9 (ZIP9) regulates zinc homeostasis in the secretory pathway: characterization of the ZIP subfamily I protein in vertebrate cells. *Biosci Biotechnol Biochem* 2009;73:1142-1148.
58. Thomas P, Pang Y, Dong J, Berg AH. Identification and characterization of membrane androgen receptors in the ZIP9 zinc transporter subfamily: II. Role of human ZIP9 in testosterone-induced prostate and breast cancer cell apoptosis. *Endocrinology* 2014;155:4250-4265.

59. Yu Y, Wu A, Zhang Z, Yan G, Zhang F, Zhang L, Shen X, et al. Characterization of the GufA subfamily member SLC39A11/Zip11 as a zinc transporter. *J Nutr Biochem* 2013;24:1697-1708.
60. Martin AB, Aydemir TB, Guthrie GJ, Samuelson DA, Chang SM, Cousins RJ. Gastric and colonic zinc transporter ZIP11 (Slc39a11) in mice responds to dietary zinc and exhibits nuclear localization. *J Nutr* 2013;143:1882-1888.
61. Langmade SJ, Ravindra R, Daniels PJ, Andrews GK. The transcription factor MTF-1 mediates metal regulation of the mouse ZnT1 gene. *J Biol Chem* 2000;275:34803-34809.
62. Palmiter RD, Findley SD. Cloning and functional characterization of a mammalian zinc transporter that confers resistance to zinc. *EMBO J* 1995;14:639-649.
63. Jirakulaporn T, Muslin AJ. Cation diffusion facilitator proteins modulate Raf-1 activity. *J Biol Chem* 2004;279:27807-27815.
64. Lazarczyk M, Pons C, Mendoza JA, Cassonnet P, Jacob Y, Favre M. Regulation of cellular zinc balance as a potential mechanism of EVER-mediated protection against pathogenesis by cutaneous oncogenic human papillomaviruses. *J Exp Med* 2008;205:35-42.
65. Andrews GK, Wang H, Dey SK, Palmiter RD. Mouse zinc transporter 1 gene provides an essential function during early embryonic development. *Genesis* 2004;40:74-81.
66. Devergnas S, Chimienti F, Naud N, Pennequin A, Coquerel Y, Chantegrel J, Favier A, et al. Differential regulation of zinc efflux transporters ZnT-1, ZnT-5 and ZnT-7 gene expression by zinc levels: a real-time RT-PCR study. *Biochem Pharmacol* 2004;68:699-709.
67. Guo L, Lichten LA, Ryu MS, Liuzzi JP, Wang F, Cousins RJ. STAT5-glucocorticoid receptor interaction and MTF-1 regulate the expression of ZnT2 (Slc30a2) in pancreatic acinar cells. *Proc Natl Acad Sci U S A* 2010;107:2818-2823.
68. Lopez V, Kelleher SL. Zinc transporter-2 (ZnT2) variants are localized to distinct subcellular compartments and functionally transport zinc. *Biochem J* 2009;422:43-52.
69. Palmiter RD, Cole TB, Findley SD. ZnT-2, a mammalian protein that confers resistance to zinc by facilitating vesicular sequestration. *EMBO J* 1996;15:1784-1791.
70. Lee S, Hennigar SR, Alam S, Nishida K, Kelleher SL. Essential Role for Zinc Transporter 2 (ZnT2)-mediated Zinc Transport in Mammary Gland Development and Function during Lactation. *J Biol Chem* 2015;290:13064-13078.

71. Salazar G, Love R, Werner E, Doucette MM, Cheng S, Levey A, Faundez V. The zinc transporter ZnT3 interacts with AP-3 and it is preferentially targeted to a distinct synaptic vesicle subpopulation. *Mol Biol Cell* 2004;15:575-587.
72. Cole TB, Wenzel HJ, Kafer KE, Schwartzkroin PA, Palmiter RD. Elimination of zinc from synaptic vesicles in the intact mouse brain by disruption of the ZnT3 gene. *Proc Natl Acad Sci U S A* 1999;96:1716-1721.
73. Huang L, Kirschke CP, Gitschier J. Functional characterization of a novel mammalian zinc transporter, ZnT6. *J Biol Chem* 2002;277:26389-26395.
74. Huang L, Gitschier J. A novel gene involved in zinc transport is deficient in the lethal milk mouse. *Nat Genet* 1997;17:292-297.
75. Kelleher SL, Lonnerdal B. Zn transporter levels and localization change throughout lactation in rat mammary gland and are regulated by Zn in mammary cells. *J Nutr* 2003;133:3378-3385.
76. Liuzzi JP, Bobo JA, Cui L, McMahon RJ, Cousins RJ. Zinc transporters 1, 2 and 4 are differentially expressed and localized in rats during pregnancy and lactation. *J Nutr* 2003;133:342-351.
77. Erway LC, Grider A, Jr. Zinc metabolism in lethal-milk mice. Otolith, lactation, and aging effects. *J Hered* 1984;75:480-484.
78. Kambe T, Narita H, Yamaguchi-Iwai Y, Hirose J, Amano T, Sugiura N, Sasaki R, et al. Cloning and characterization of a novel mammalian zinc transporter, zinc transporter 5, abundantly expressed in pancreatic beta cells. *J Biol Chem* 2002;277:19049-19055.
79. Fukunaka A, Suzuki T, Kurokawa Y, Yamazaki T, Fujiwara N, Ishihara K, Migaki H, et al. Demonstration and characterization of the heterodimerization of ZnT5 and ZnT6 in the early secretory pathway. *J Biol Chem* 2009;284:30798-30806.
80. Inoue K, Matsuda K, Itoh M, Kawaguchi H, Tomoike H, Aoyagi T, Nagai R, et al. Osteopenia and male-specific sudden cardiac death in mice lacking a zinc transporter gene, Znt5. *Hum Mol Genet* 2002;11:1775-1784.
81. Ohana E, Hoch E, Keasar C, Kambe T, Yifrach O, Hershinkel M, Sekler I. Identification of the Zn<sup>2+</sup> binding site and mode of operation of a mammalian Zn<sup>2+</sup> transporter. *J Biol Chem* 2009;284:17677-17686.
82. Huang L, Yu YY, Kirschke CP, Gertz ER, Lloyd KK. Znt7 (Slc30a7)-deficient mice display reduced body zinc status and body fat accumulation. *J Biol Chem* 2007;282:37053-37063.
83. Kirschke CP, Huang L. ZnT7, a novel mammalian zinc transporter, accumulates zinc in the Golgi apparatus. *J Biol Chem* 2003;278:4096-4102.

84. Chimienti F, Devergnas S, Pattou F, Schuit F, Garcia-Cuenca R, Vandewalle B, Kerr-Conte J, et al. In vivo expression and functional characterization of the zinc transporter ZnT8 in glucose-induced insulin secretion. *J Cell Sci* 2006;119:4199-4206.
85. Pound LD, Hang Y, Sarkar SA, Wang Y, Milam LA, Oeser JK, Printz RL, et al. The pancreatic islet beta-cell-enriched transcription factor Pdx-1 regulates Slc30a8 gene transcription through an intronic enhancer. *Biochem J* 2011;433:95-105.
86. Pound LD, Sarkar SA, Benninger RK, Wang Y, Suwanichkul A, Shadoan MK, Printz RL, et al. Deletion of the mouse Slc30a8 gene encoding zinc transporter-8 results in impaired insulin secretion. *Biochem J* 2009;421:371-376.
87. Chimienti F, Devergnas S, Favier A, Seve M. Identification and cloning of a beta-cell-specific zinc transporter, ZnT-8, localized into insulin secretory granules. *Diabetes* 2004;53:2330-2337.
88. Sim DL, Chow VT. The novel human HUEL (C4orf1) gene maps to chromosome 4p12-p13 and encodes a nuclear protein containing the nuclear receptor interaction motif. *Genomics* 1999;59:224-233.
89. Chen YH, Kim JH, Stallcup MR. GAC63, a GRIP1-dependent nuclear receptor coactivator. *Mol Cell Biol* 2005;25:5965-5972.
90. Liuzzi JP, Cousins RJ. Mammalian zinc transporters. *Annu Rev Nutr* 2004;24:151-172.
91. Fujishiro H, Yoshida M, Nakano Y, Himeno S. Interleukin-6 enhances manganese accumulation in SH-SY5Y cells: implications of the up-regulation of ZIP14 and the down-regulation of ZnT10. *Metallomics* 2014;6:944-949.
92. Patrushev N, Seidel-Rogol B, Salazar G. Angiotensin II requires zinc and downregulation of the zinc transporters ZnT3 and ZnT10 to induce senescence of vascular smooth muscle cells. *PLoS One* 2012;7:e33211.
93. Bosomworth HJ, Thornton JK, Coneyworth LJ, Ford D, Valentine RA. Efflux function, tissue-specific expression and intracellular trafficking of the Zn transporter ZnT10 indicate roles in adult Zn homeostasis. *Metallomics* 2012;4:771-779.
94. Leyva-Illades D, Chen P, Zogzas CE, Hutchens S, Mercado JM, Swaim CD, Morrisett RA, et al. SLC30A10 is a cell surface-localized manganese efflux transporter, and parkinsonism-causing mutations block its intracellular trafficking and efflux activity. *J Neurosci* 2014;34:14079-14095.
95. Homer WJ. The histogenesis of the blood platelets. *Journal of Morphology* 1910;21:263-278.



96. Deutsch VR, Tomer A. Advances in megakaryocytopoiesis and thrombopoiesis: from bench to bedside. *Br J Haematol* 2013;161:778-793.
97. Ru YX, Zhao SX, Dong SX, Yang YQ, Eyden B. On the maturation of megakaryocytes: a review with original observations on human in vivo cells emphasizing morphology and ultrastructure. *Ultrastruct Pathol* 2015;39:79-87.
98. Machlus KR, Italiano JE, Jr. The incredible journey: From megakaryocyte development to platelet formation. *J Cell Biol* 2013;201:785-796.
99. Schulze H, Korpal M, Hurov J, Kim SW, Zhang J, Cantley LC, Graf T, et al. Characterization of the megakaryocyte demarcation membrane system and its role in thrombopoiesis. *Blood* 2006;107:3868-3875.
100. Gremmel T, Frelinger AL, 3rd, Michelson AD. Platelet Physiology. *Semin Thromb Hemost* 2016;42:191-204.
101. Marx G, Korner G, Mou X, Gorodetsky R. Packaging zinc, fibrinogen, and factor XIII in platelet alpha-granules. *J Cell Physiol* 1993;156:437-442.
102. Sharda A, Flaumenhaft R. The life cycle of platelet granules. *F1000Res* 2018;7:236.
103. Hitchcock IS, Kaushansky K. Thrombopoietin from beginning to end. *Br J Haematol* 2014;165:259-268.
104. Schulze H. Culture, Expansion, and Differentiation of Murine Megakaryocytes from Fetal Liver, Bone Marrow, and Spleen. *Curr Protoc Immunol* 2016;112:22F 26 21-22F 26 15.
105. Rahman MT, De Ley M. Metallothionein in human thrombocyte precursors, CD61+ megakaryocytes. *Cell Biol Toxicol* 2008;24:19-25.
106. Mahdi F, Madar ZS, Figueroa CD, Schmaier AH. Factor XII interacts with the multiprotein assembly of urokinase plasminogen activator receptor, gC1qR, and cytokeratin 1 on endothelial cell membranes. *Blood* 2002;99:3585-3596.
107. Bernardo MM, Day DE, Olson ST, Shore JD. Surface-independent acceleration of factor XII activation by zinc ions. I. Kinetic characterization of the metal ion rate enhancement. *J Biol Chem* 1993;268:12468-12476.
108. Baglia FA, Gailani D, Lopez JA, Walsh PN. Identification of a binding site for glycoprotein Ibalpha in the Apple 3 domain of factor XI. *J Biol Chem* 2004;279:45470-45476.
109. Gordon PR, Woodruff CW, Anderson HL, O'Dell BL. Effect of acute zinc deprivation on plasma zinc and platelet aggregation in adult males. *Am J Clin Nutr* 1982;35:113-119.

110. Emery MP, Browning JD, O'Dell BL. Impaired hemostasis and platelet function in rats fed low zinc diets based on egg white protein. *J Nutr* 1990;120:1062-1067.
111. Heyns Adu P, Eldor A, Yarom R, Marx G. Zinc-induced platelet aggregation is mediated by the fibrinogen receptor and is not accompanied by release or by thromboxane synthesis. *Blood* 1985;66:213-219.
112. O'Dell BL. Role of zinc in plasma membrane function. *J Nutr* 2000;130:1432S-1436S.
113. Vu TT, Fredenburgh JC, Weitz JI. Zinc: an important cofactor in haemostasis and thrombosis. *Thromb Haemost* 2013;109:421-430.
114. Marx G. Zinc binding to fibrinogen and fibrin. *Arch Biochem Biophys* 1988;266:285-288.
115. Marx G, Hopmeier P, Gurfel D. Zinc alters fibrin ultrastructure. *Thromb Haemost* 1987;57:73-76.
116. Kiran Gotru S, van Geffen JP, Nagy M, Mammadova-Bach E, Eilenberger J, Volz J, Manukjan G, et al. Defective Zn(2+) homeostasis in mouse and human platelets with alpha- and delta-storage pool diseases. *Sci Rep* 2019;9:8333.
117. Franklin RB, Ma J, Zou J, Guan Z, Kukoyi BI, Feng P, Costello LC. Human ZIP1 is a major zinc uptake transporter for the accumulation of zinc in prostate cells. *J Inorg Biochem* 2003;96:435-442.
118. Cousins RJ, Blanchard RK, Popp MP, Liu L, Cao J, Moore JB, Green CL. A global view of the selectivity of zinc deprivation and excess on genes expressed in human THP-1 mononuclear cells. *Proc Natl Acad Sci U S A* 2003;100:6952-6957.
119. Tsuda M, Imaizumi K, Katayama T, Kitagawa K, Wanaka A, Tohyama M, Takagi T. Expression of zinc transporter gene, ZnT-1, is induced after transient forebrain ischemia in the gerbil. *J Neurosci* 1997;17:6678-6684.

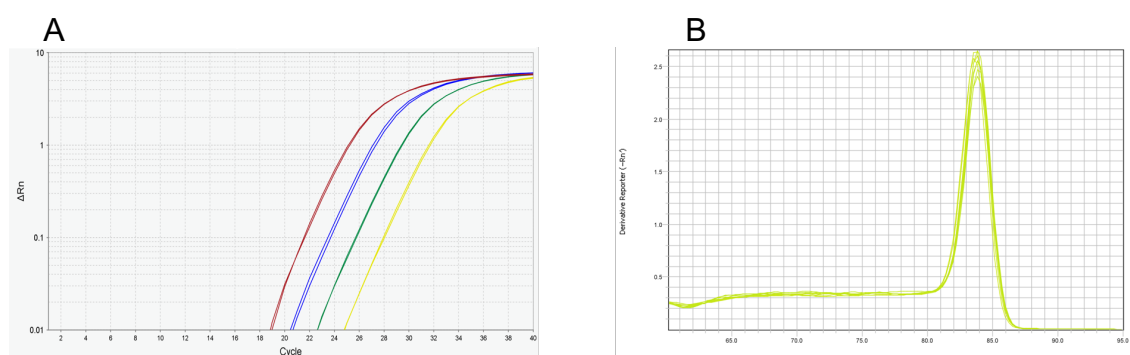
## 7. List of Figures

Figure 1. Dysregulated zinc uptake or release induces multiple defects in several organs of the human body. ....	2
Figure 2. Schematic picture of metallothionein thiolate clusters binding to Zn <sup>2+</sup> . ....	4
Figure 3. Subcellular localization of selected ZIP and ZnT transporters in mammalian cells. ....	6
Figure 4. Characterization of cultivated murine megakaryocytes. ....	28
Figure 5. Effects of extracellular ZnCl <sub>2</sub> in megakaryocytes. ....	29
Figure 6. Zinc chelation reduces survival rate of primary mouse megakaryocytes. ....	30
Figure 7. Relative mRNA expression as determined by C <sub>T</sub> values of <i>Slc39a</i> genes encoding ZIP transporters. ....	32
Figure 8. Relative mRNA expression of <i>Slc39a1</i> (ZIP1) in mouse MKs. ....	34
Figure 9. Relative mRNA expression of <i>Slc39a3</i> (ZIP3) in mouse MKs. ....	35
Figure 10. Relative mRNA expression of <i>Slc39a4</i> (ZIP4) in mouse MKs. ....	36
Figure 11. Relative mRNA expression of <i>Slc39a6</i> (ZIP6) in mouse MKs. ....	37
Figure 12. Relative mRNA expression of <i>Slc39a7</i> (ZIP7) in mouse MKs. ....	38
Figure 13. Relative mRNA expression of <i>Slc39a9</i> (ZIP9) in mouse MKs. ....	39
Figure 14. Relative mRNA expression of <i>Slc39a10</i> (ZIP10) in mouse MKs. ....	41
Figure 15. Relative mRNA expression of <i>Slc39a11</i> (ZIP11) in mouse MKs. ....	42
Figure 16. Relative mRNA expression as determined by C <sub>T</sub> values of <i>Slc30a</i> genes encoding ZnT transporters. ....	43
Figure 17. Relative mRNA expression of <i>Slc30a1</i> (ZnT1) in mouse MKs. ....	45
Figure 18. Relative mRNA expression of <i>Slc30a5</i> (ZnT5) in mouse MKs. ....	46
Figure 19. Relative mRNA expression of <i>Slc30a6</i> (ZnT6) in mouse MKs. ....	47
Figure 20. Relative mRNA expression of <i>Slc30a7</i> (ZnT7) in mouse MKs. ....	48
Figure 21. Relative mRNA expression of <i>Slc30a9</i> (ZnT9) in mouse MKs. ....	49
Figure 22. Successful RT-PCR with <i>Slc39a1</i> primer and cDNA derived from mouse liver tissue. ....	71

## 8. Appendix

### 8.1 RT-PCR primer test based on the example of *Slc30a1* in liver tissue

For the analysis of gene transcription in the present study, RT-PCR was used (see chapter 2.2.11). All primers for analysis of gene expression in this study were tested for performance and specificity. In the following, the procedure is shortly presented based on the example of *Slc39a1*. The full primer test data can be requested from the author of the present study.



**Figure 22. Successful RT-PCR with *Slc39a1* primer and cDNA derived from mouse liver tissue.** (A) Amplification Plot. cDNA samples of different dilutions in nuclease free water were used in duplicates, resulting in shifted Amplification curves. From left to right: Undiluted (red), 1/4 dilution (blue), 1/16 dilution (green) and 1/64 dilution (yellow). (B) Melt curve plot. PCR products of all cDNA dilutions were heated and melting temperatures of the double strands were recorded.

Performance of RT-PCR primers was tested using a cDNA sample with reportedly high expression of the requested gene. In the case of *Slc39a1*, cDNA derived from liver tissues was used. Then, RT-PCR was performed with different dilutions of the cDNA sample and the  $C_T$  value of each dilution was recorded. When primer performance reaches 100%, which means that every requested target DNA is amplified per PCR cycle, the  $C_T$  value should match with the difference in cDNA concentration of the sample. On the example of *Slc39a1*,  $\Delta C_T$  values between dilutions of  $\frac{1}{2^n}$  matched the value of  $n$ , indicating good performance of the primer pair (Fig. 22A).

To ensure primer specificity, the RT-PCR product is heated and the melting temperature where the double stranded DNA breaks into single strands is

recorded. If the product is free from nonsense copies, only one melting peak should appear. In this example (Fig. 22B) one can assume that the measured fluorescence amplification originates from the requested Slc39a1 cDNA sequence.

## 8.2 Publication

The author contributed to the following publication:

“Defective Zn<sup>2+</sup> homeostasis in mouse and human platelets with  $\alpha$ - and  $\delta$ -storage pool diseases.”

Gotru KS, van Geffen JP, Nagy M, Mammadova-Bach E, Eilenberger J, Volz J, Manukjan G, Schulze H, Wagner L, Eber S, Schambeck C, Deppermann C, Brouns S, Nurden P, Greinacher A, Sachs U, Nieswandt B, Hermanns HM, Heemskerk JWM, Braun A.

Sci Rep. 2019 Jun 6;9(1):8333. doi: 10.1038/s41598-019-44751-w”

## **Acknowledgement**

I would like to thank Prof. Dr. med. Andreas Geier for his supervision during my work on this thesis.

I would like to thank Dr. Attila Braun for his help with cell culture, for the ideas that drove this work forward as well as his patience with my attempts in scientific writing.

I am grateful to PD Dr. Heike Hermanns for the warm welcome in her lab and her support during my work, as well as Dr. Daniel Jahn and Donata Dorbath for their comprehensive explanations.

And last but not least: Thank you Daria and thank you to my family for your constant motivation.

This study was supported by the Deutsche Forschungsgemeinschaft project number 374031971-TRR 240/A09 to Dr. Attila Braun and PD Dr. Heike M. Hermanns

## ***Curriculum vitae***

Name Leonard Wagner

Geburtsort Leipzig

Nationalität Deutsch

### **Ausbildung**

08/2016 – 2019 Promotionsarbeit an der Klinik und Poliklinik für  
Medizin II Würzburg, Abteilung Hepatologie

12/2018 Approbation als Zahnarzt

10/2013 - 11/2018 Studium der Zahnmedizin an der  
Julius-Maximilians-Universität Würzburg  
Abschluss mit Staatsexamen

2005-2013 Burghardt-Gymnasium Buchen  
Abschluss mit Abitur

2001-2005 Wimpina-Grundschule Buchen